C.P. No. 1308

C.P. No. 1308

PROCUREMENT EXECUTIVE, MINISTRY OF DEFENCE

AERONAUTICAL RESEARCH COUNCIL

CURRENT PAPERS

The Prediction of Boundary-Layer Behaviour and Profile Drag for Infinite Yawed Wings:

Part II Flow Near a Turbulent Attachment Line

by

B. G. J. Thompson

Aerodynamics Dept., R.A.E., Teddington

LIBRARY
ROYAL AIRCRAFT ESTABLISHMENT
BEDFORD.

LONDON: HER MAJESTY'S STATIONERY OFFICE

1974

PRICE *£1 - 10* NET

UDC 533.693.1 ; 532.526 ; 532.526.4 : 533.6.013.122 : 533.6.013.154

* CP No.1308
May 1973

THE PREDICTION OF BOUNDARY-LAYER BEHAVIOUR AND PROFILE DRAG FOR INFINITE YAWED WINGS:

Part II FLOW NEAR A TURBULENT ATTACHMENT LINE

by

B. G. J. Thompson **

SUMMARY

In the region of strong favourable pressure gradient between the leading-edge attachment line and the pressure minimum, comparisons with the measurements of Cumpsty and Head[1], on a 62.5° swept wing, show that current turbulent boundary-layer methods[2,3] do not predict the boundary layer growth accurately enough for practical design applications. Physically, the conditions are severe as there are strong cross-flows developing in the presence of large wall curvature.

Calculations, using the entrainment method of Ref.4. show that, even at flight Reynolds numbers, a conventional swept wing with turbulent attachment line flow could be affected by a prolonged region of reverse transition. Simple assumptions are used to estimate the effect of this on boundary-layer development. It is found that the profile drag could be affected by several per cent and it is thought that the shock-induced separation and scale effects for 'peaky' transonic aerofoils would be even more susceptible to the presence of laminar reversion and that the use of an attachment line criterion for turbulent flow (such as C*) is inadequate on its own.

Finally, calculations using the same boundary-layer method are employed to provide charts from which a basic experiment at low speeds can be designed to investigate these problems on a yawed circular cylinder (suitably faired). Results are provided for the 13ft × 9ft wind tunnel at RAE Bedford and for the 5ft × 4ft wind tunnel at the Cambridge University Engineering Laboratory.

---

* Replaces RAE Technical Report 73091 - ARC 35095

** Now with the DOE, CEDAR project, PCAO (DBD), Lunar House, Croydon

CONTENTS

1 INTRODUCTION

The flow along the leading-edge attachment lines of swept wings has been investigated by several authors in laminar[5,6,8], in transitional[6,7,8], and also in fully turbulent flow[1,9,10]. There has also been a large amount of theoretical[2,3,11] and some experimental[12,13,14,15] work carried out on three-dimensional turbulent boundary layers in zero or adverse pressure gradient conditions such as might be found well downstream of the leading-edge region of a real swept wing. Unfortunately, from the point of view of the designer of a swept wing, where the attachment line flow may be fully turbulent in flight conditions, there appears to be no information available either in the form of direct experimental measurements of boundary layer behaviour or in the form of theoretical predictions for the remaining region of (favourable pressure gradient) flow lying between the partial stagnation line and the locus of the leading-edge pressure minimum.

That there is a practical requirement for a better understanding of the flow in this region is demonstrated by the present results, shown in Figs.1 to 3, for the Cumpsty-Head wing[12]. The turbulent boundary layer calculations started from the attachment line lead to values of θ_{11}, H_{11} and β, at the 'peak' velocity position ($x'/c' = 0.21$), which differ from the measurements. This difference leads in turn to markedly different predictions for the development of boundary layer properties in the region of adverse pressure gradient, and of the position of rear separation, from those calculations started with the measured values at the 'peak'. This is a feature not only of the entrainment method described in Part I[4] of the present series of papers but also of the turbulence energy method[3].

The foregoing difficulties are mentioned in Part III of the present series of Reports[16], where the possibility of reverse transition occurring, even at flight Reynolds numbers, in the leading-edge region is also briefly indicated. The present paper elaborates somewhat upon both of these aspects and suggests that one of the most urgent pieces of fundamental work needed at the present time may well be an investigation of this region.

The flow is likely to be a complex one, physically, and may lead, especially for aerofoils with large leading-edge 'peaks', to significant uncertainties in the predictions of profile drag, rear separation, viscous displacement effect and of other quantities of practical interest obtained from any calculation method for swept wings in viscous, compressible flow such as proposed in Ref.17.

In sections 3.3, 3.4, two infinite yawed wings with sections and pressure distributions of a practical nature are examined in some detail by means of parametric calculations made using the entrainment method of Part I[4]. The first wing employs an 18% thick RAE 101 chordwise section at low speed ($M_\infty \cos \Lambda = 0.1$) and with $\alpha \sec \Lambda = 8.32^\circ$. It has a moderate leading-edge peak and fully attached flow. The second wing has the RAE (NPL) 3111 section at its design flat roof-top condition ($M_\infty \cos \Lambda = 0.665$ $C_L \sec^2 \Lambda = 0.515$) examined[16] in Part III of the present series of Reports. For both wings, it is found that a significant range of flight conditions would be affected by prolonged regions of reverse transition. Crude estimates are made, for the RAE 101 section, which suggests that the level of upper surface profile drag may be lowered by as much as 8 per cent from the fully turbulent value if reverse transition is present; the exact amount depending on the extent of the relaminarized flow.

Finally, in the Appendix, design charts are presented from which it is possible rapidly to assess the feasibility of using a yawed circular cylinder as the basis of a boundary-layer experiment, in a low-speed wind tunnel, to examine both the fully turbulent boundary layer and the conditions of reverse transition downstream of swept leading edges. Outline calculations are given for the 13ft × 9ft wind tunnel at RAE Bedford and for the 5ft × 4ft wind tunnel at the Cambridge University Engineering Laboratory.

The importance of understanding and of predicting accurately this leading-edge flow is comparable with that of predicting transition in two-dimensions. For instance, if the flow is turbulent initially on the swept attachment line, by virtue of contamination from the fuselage boundary layer, then the occurrence or otherwise of a region of reverse transition (resulting in a laminar state at the velocity peak) would lead to markedly different behaviour of vortex separations or leading-edge bubbles and of course any boundary-layer/shock interactions would be severely affected*. Consequently, it is extremely important to improve our knowledge of this region especially when it is remembered that use of 'peaky' sections[25], with large values of C*, could give rise to flows that are more sensitive to these uncertainties, than the flow about more conventional sections, at cruise**.

---

* This paper can only serve to draw attention to these uncertainties: at the present time it would be difficult to attempt reliable predictions of their magnitudes.

** It is assumed that we are able in practice to consider a smooth leading-edge surface. As supercritical sections are likely to be more critical as regards shape and surface finish than conventional sections this seems to be a reasonable assumption.

For off-design conditions, especially with powerful leading-edge devices, the likelihood of turbulent attachment line flow and of laminar reversion before the 'peak' seems even greater than at cruise. The situation, from the wing design point of view, is further complicated by the uncertain accuracy of present day approximate methods of predicting detailed potential flow pressure distributions around the leading edges of finite swept wings, especially in compressible flow[17]. The position of the attachment line itself may not be known accurately, especially near to the apex of the wing.

The question that remains to be answered is therefore: 'Are the levels of inaccuracies due to the boundary layer predictions swamped by the inaccuracies due to the potential flow calculations or are they both large enough to require further work?'

The answer to this question is beyond the scope of the present series of papers but it is believed that some useful indication of the uncertainties in the boundary-layer predictions is provided by the observations given here. These observations can be regarded as an extension to the list of possible difficulties facing the designer in viscous three-dimensional flow, that was collected recently by Hall[18] in his review paper.

2 FULLY TURBULENT FLOW ON SWEPT WINGS

2.1 Comparison of turbulent boundary-layer predictions with measurements on the Cumpsty-Head 62.5° wing

Results of calculations for the boundary-layer growth behind the pressure minimum on this infinite yawed wing have been presented elsewhere[3,12] but, at the start of the present investigation, no attempt had been made to predict the complete boundary-layer starting from the leading-edge attachment line. It was important to attempt this because the design of swept wings in viscous flow necessitates[17] full chord predictions, no values of boundary-layer properties being available, at the locus of pressure minima, to start the boundary-layer calculation.

Two different boundary-layer methods were available, namely:

(1) the turbulence energy method of Bradshaw[3] and,

(2) the entrainment integral method presented in Part I of the present series of Reports[4]. This method is used, in Part III of this series (see Ref.16), to investigate the influence of sweep on profile drag and rear separation behaviour for a realistic family of yawed wings.

Using either method, predictions have been obtained for flow along turbulent attachment lines and also in three-dimensional boundary layers with zero or adverse pressure gradients. However, numerical problems occur in the strong favourable pressure gradients that characterise the leading-edge region. Also, numerically, some method must be found to advance the calculation from the attachment line itself.

Ref.4 shows how these problems were satisfactorily overcome for the entrainment method and the calculations in the present Report use this method throughout, except (in this section) for a few results obtained from the turbulence energy method for the Cumpsty-Head wing. The latter calculations were started from initial values, just downstream of the attachment line, found by using the entrainment method.

Pressure distribution (B) of Fig.9 in Ref.4 was used for the calculations. The results of the present predictions, started from the leading edge and from the pressure minimum ($x'/c' = 0.21$), are compared in Figs.1, 2 and 3 for θ_{11}/c', H_{11} and β, respectively. A sweep angle of $\Lambda = 62.5^{\circ}$ was assumed. Further details of the entrainment calculations can be found in Ref.4 where, for example, the individual terms in the equations are plotted out across the complete boundary-layer development.

From Fig.1, it is clear that starting either method from the (measured) attachment line values results in a considerable underestimation of momentum growth as separation (measured at $x'/c' = 0.86$) is approached, whereas the calculations started at the 'peak' agree well with experiment.

Similarly, the streamwise shape-factor (H_{11}) grows less rapidly if the prediction is started from the leading-edge (see Fig.2). The initial transients in Bradshaw's result are due to the difficulty of estimating initial shear stress profiles in three-dimensional conditions.

From the above it may be inferred that quantities of practical importance to the designer (such as momentum thickness and displacement thickness) are surprisingly sensitive to the position from which the calculations are started, although the values of H_{11} and θ_{11}/c' at the beginning of the adverse pressure gradient seem to be nearly independent of starting position. However, the development of cross-flow properties is affected more noticeably as seen in Fig.3, where the surface cross-flow angle (β) at $x'/c' = 0.21$, predicted from calculations started at the leading-edge, is more than twice the magnitude of the measured value used to start the other calculations.

2.2 Discussion

The effects of favourable pressure gradient on the inner region of the mean velocity profile are considered later (in section 3.1) where it is suggested that turbulent flow would break down if

$$\Delta_{1s} \leqslant -0.01 \quad , \qquad (1)$$

where $\Delta_{1s} = \frac{\nu_w}{u_\tau^3} \frac{1}{\rho_w} \left(\frac{(\text{grad } \underline{p} . \underline{\tau_w})}{|\underline{\tau_w}|} \right)$ and

where the term in brackets is the component of the pressure gradient vector taken in the direction of the surface shear vector ($\underline{\tau_w}$). However, according to the calculations, this value is never reached in the experimental condition considered here and although $R_{\theta_{11}}$ falls from a value of 620, on the attachment line itself, to about 250 just downstream, it rises rapidly again and hence the flow can probably be regarded as fully turbulent everywhere. Consequently, reverse transition does not explain the disagreement between theory and experiment in the leading-edge region.

In order to make predictions of sufficient accuracy for swept wing design it is necessary to carry out experiments to provide fundamental data to calibrate boundary-layer methods in this difficult region.

The foregoing results reveal the present problems for (nominally) fully turbulent flow everywhere, but subsequent calculations showed that even in flight conditions on sections of a more practical type there were strong indications, from the calculations, that reverse transition could occur, thereby creating further uncertainty regarding the accuracy of turbulent boundary-layer predictions. These aspects are examined in the following sections, and the design of a suitable experiment is considered in the Appendix.

3 REVERSE TRANSITION NEAR SWEPT LEADING-EDGES

3.1 Criteria for reverse transition

In two-dimensional and axisymmetric flow Patel[19] showed that if

$\Delta_1 = \left(\frac{\nu}{u_\tau^3} \frac{1}{\rho} \frac{dp}{dx} \right) < -0.01$ approximately, then the turbulent inner region broke down and reverse transition could start. Launder[20] further suggested, on the basis of his own measurements, that this condition of strong favourable pressure gradient must be maintained for a streamwise distance of about twenty mean boundary-layer thicknesses (δ_{AV}) before laminar flow could become established.

In three-dimensional flow, the parameter corresponding to Δ_1 for the inner region with cross-flow is Δ_{1s}, given by equation (1). For an infinite yawed wing the expression simplifies to

$$\Delta_{1s} = \frac{\nu_w}{U_\tau^3} \frac{1}{\rho_w} \frac{dp}{ds'} \cos(\phi + \beta) \quad , \qquad (2)$$

where $\frac{dp}{ds'}$ is the pressure gradient chordwise, ϕ and β are defined in Fig.4.

3.2 <u>The method of boundary-layer calculation</u>

For fully turbulent flow $(\Delta_{1s} > -0.01)$ the entrainment method (see Ref.1) used throughout the remainder of the present paper employs the entrainment function $F(H_1)$ as originally proposed by Head[21], together with the compressibility assumptions of Green[22].

Once laminar reversion is indicated $(\Delta_{1s} \leqslant -0.01)$ the entrainment is set to zero (F = 0) since in quasi-laminar flow the mixing intensity is expected to be very much less than the turbulent value. This is obviously an extremely oversimplified view of the complicated physics of the situation but represents fairly honestly the poor current level of knowledge especially in three-dimensional flow. However, this simple assumption should give a reasonable estimate of the magnitude of the effects due to reverse transition by comparison with results using $F(H_1)$ throughout.

The length along an external streamline for which $\Delta_{1s} \leqslant -0.01$, is taken as the extent of laminar reversion and is called L_{RT}. Hence Launder's condition is used in the form:

$$L_{RT} \geqslant 20\delta_{AV} \quad . \qquad (3)$$

3.3 <u>Calculations of boundary-layer behaviour in the leading-edge region of a 60° swept wing having a symmetrical section at incidence</u>

The wing considered here has a chordwise section (normal to its leading edge) of 18% RAE 101 and the operating conditions are $M_\infty \cos\Lambda = 0.1$, $\alpha \sec\Lambda = 8.32°$ expressed in the form appropriate to infinite yawed wings (see Ref.16, for example). The streamwise chord Reynolds number is $R_c = 4.6 \times 10^6$.

These conditions correspond to one of the conditions studied by Garner[23] during his experiments in the 13ft × 9ft tunnel at NPL. His results were confined to flow visualisation and surface static pressure distributions because of the small size of the models tested. The measured pressure distribution at $\eta = 0.555$ was used for the present calculations as it was in a region where infinite yawed wing conditions occurred.

The flow around the leading-edge region is displayed in some detail in Fig.5. The lowest diagram shows a section normal to the leading edge where it is seen that the stagnation point is well below the geometric leading edge and hence that there is a considerable length of surface around the leading edge from the stagnation point to the pressure minimum. This is shown in the middle sketch where the strong favourable chordwise pressure gradient gives rise to laminar reversion between $s'/c' = 0.012$ and 0.056. This corresponds (see upper diagram) to $\Delta_{1s} \leqslant -0.01$ for a length of $L_{RT} = 50\delta_{AV}$ along the path of the external streamline.

The boundary-layer predictions shown in the upper figure reveal a significant difference between the momentum thickness at the pressure minimum as obtained from the fully turbulent results ($R_{\theta_{11}} = 440$) and that from the calculation for laminar reversion ($R_{\theta_{11}} = 200$). This difference in initial values at the beginning of the adverse pressure gradient results in a 4% difference in upper surface profile drag. That is:

$$\text{with laminar reversion,} \quad C_{D_u} = 0.00417, \text{ and}$$

$$\text{fully turbulent flow,} \quad C_{D_u} = 0.00434.$$

The corresponding results for streamwise shape factor (H_{11}) development and surface cross flow angle (β) are shown in Figs.6 and 7.

Despite the crude nature of the zero entrainment assumption the predictions are qualitatively reasonable as, in quasi-laminar flow, the reduced mixing should result in increased cross flow and a shape factor which rises towards the laminar value.

The significance of $H_{11} > 2.4$ (say) is not easily assessed but indicates that separation would be rather more likely after the pressure minimum is passed if laminar reversion takes place than if the flow were everywhere turbulent ($H_{11} < 1.5$ say).

3.4 Calculations for a family of infinite yawed wings based on a lowspeed symmetrical aerofoil at incidence

The conditions first considered (above) led to a parametric study of a family of infinite yawed wings with the same section operating at these conditions of $M_\infty \cos \Lambda = 0.1$, $\alpha \sec \Lambda = 8.32^o$, but over a range of Λ and R_c. The results are shown in Fig.8 as two families of curves:

(i) Contours of the ratio L_{RT}/δ_{AV} for which the flow is expected to undergo reverse transition $(\Delta_{1s} \leqslant - 0.01)$ on the upper surface, and

(ii) contours of constant percentage reduction in upper surface profile drag $(100\ \Delta C_{D_u}/C_{D_u})$ due to laminar reversion.

If $C^* = 7 \times 10^4$ is assumed to be the condition for the change from laminar to turbulent attachment line flow then a considerable range of flight Reynolds numbers and sweep angles are affected by the uncertainties due to possible laminar reversion. For example, a typical flight condition appropriate to low Mach number and moderate sweep with a moderate C_L produced by incidence rather than by camber might be:

$$\Lambda = 30^o, \quad R_c = 2 \times 10^7, \quad C^* \simeq 1 \times 10^5, \quad C_L \simeq 0.6, \quad M_\infty \simeq 0.11.$$

At this condition, the predictions indicate that the effect of laminar reversion is to give a reduction of as much as 6% in C_{D_u}. This is large enough to be of considerable practical interest to the designer.

If $C^* = 1.4 \times 10^5$ is used, then the range is much reduced but the effect on profile drag of reverse transition is still of the order of 2 to 3% for an aerofoil which, in this example, is not operating under severe conditions.

As a rough rule, values of $C^* \geqslant 2.2 \times 10^5$ indicate full chord turbulent flow for this family of wings, at this operating condition, as then $L_{RT} \leqslant 20\delta_{AV}$.

However, the aerofoil considered is not representative of a modern section designed for good performance at a transonic cruise condition and so an additional investigation was made of the family of infinite yawed wings studied by Thompson, Carr-Hill and Ralph[16] in Part III of the present series of papers.

3.5 Calculations for the family of infinite yawed wings using a rooftop aerofoil

This family of wings (see Ref.16) employed the RAE (NPL) 3111 section in the chordwise plane, operating at its design (sonic) flat rooftop condition of:

$$M_\infty \cos \Lambda = 0.665 \ ,$$

and

$$C_L \sec^2 \Lambda = 0.515 \ . \tag{4}$$

Calculations were made using the assumption of zero entrainment and the results are shown in Fig.9, where contours of L_{RT}/δ_{AV} are plotted in the $\log_{10} R_c$ *versus* Λ plane. Unfortunately, insufficient time was available to complete the investigation by evaluating the effect on profile drag. However, there is ample confirmation of the likelihood of reverse transition occurring at flight conditions of practical interest. For example, taking the condition,

$$\Lambda = 35^\circ, \quad R_c = 40 \times 10^6, \quad \text{(see Fig.9)},$$

typical of medium to large transonic transport aircraft such as the A-300B Airbus, it seems likely that, if the leading-edge conditions were similar to those of the RAE (NPL) 3111 section at cruise then a length of about $150\delta_{AV}$ of boundary layer would be available in which reverse transition could establish itself.

The much larger aircraft typified by the Lockheed C-5A are however unlikely to be affected by reverse transition as, for instance at:

$$\Lambda = 35^\circ, \quad R_c = 1 \times 10^8 \ \text{(see Fig.9)}, \quad L_{RT} \simeq 15\delta_{AV} \ .$$

4 DISCUSSION

4.1 The physical environment near a swept leading edge

The conditions are difficult for a boundary-layer calculation because:

(i) The Reynolds numbers will be low. For example, in the case of RAE (NPL) 3111 studied above, $R_{\theta_{11}}$ falls to a minimum value lying between 250 and 1000 depending on sweep and R_c.

(ii) There is a strong favourable pressure gradient.

(iii) The surface curvature parameter (δ/R_0) in the plane of the surface shear vector $(\underline{\tau_w})$, where $R_0 = R/\cos^2(\phi + \beta)$, and R is local surface curvature in the chordwise plane, can rise to a value as high as 0.03 (see Fig.14 for a cylindrical leading edge). This value is an order of magnitude larger than that suggested by Bradshaw[24] for onset of significant curvature effects.

(iv) There is a strong divergence of the external streamlines, and finally,

(v) the cross flow can become large and varies rapidly as the boundary layer develops (see Fig.7, for example).

Any one of the above factors would make turbulent boundary-layer prediction difficult in fully turbulent conditions. Taken together, and especially if the flow has a transitional nature, the confidence that can be placed in current methods, all of which require calibration for their empirical factors, must be quite low until fresh data are acquired from an experiment such as that suggested in the Appendix.

4.2 The use of the present assumptions in compressible flow

The transition region lengthens rapidly as compressibility effects increase the resistance of the laminar flow to the growth of disturbances. This means that if laminar flow is established, as suggested by the present calculations, despite contamination of the leading edge by the fuselage boundary layer, then it is likely to persist farther and increase the likelihood of unfavourable interactions with any shock waves that may be present near the pressure minimum. Also the reverse transition process itself may be hastened by the stabilising effect of compressibility although these observations are only speculative at this stage.

4.3 Practical consequences for designs having more modern wing sections

In Fig.10, three rather different sections with different operating conditions are compared. The distributions of chordwise component of external velocity around their leading-edges are plotted as functions of surface distance from stagnation.

Curves (A) and (B) correspond to the RAE 101 and the RAE (NPL) 3111 sections previously considered. Curve (C) is taken from measurements on an advanced NLR 'peaky' section designed, using the theory of Ref.25, to operate with shock-free supersonic flow over a significant proportion of its chord. It is seen that such a section differs from the more conventional aerofoils by:

(1) A larger leading-edge radius giving rise to an initially smaller chordwise velocity gradient $\left[\frac{dU_1/U_\infty \cos\Lambda}{ds'/c'}\right]_{a.l.}$ and hence a larger effective leading-edge radius of $\sigma' = 0.106c'$. Hence, larger values of C^*, at a given Λ and R_c, are associated with this aerofoil and so there is a greater range of operating conditions for which the swept attachment line flow will be fully turbulent.

(2) There is a greater distance between stagnation and the velocity peak, and

(3) the favourable pressure gradient increases steadily until just before the peak.

Condition (3) makes the onset of reverse transition more likely compared to orthodox sections and the condition (2) ensures that once it starts it is more likely to be completed. Finally,

(4) the peak itself is sharper than conventional sections and the local Mach number is higher, consequently separation bubbles and adverse laminar or transitional interactions with shocks (off-design) are more probable.

5 CONCLUSIONS AND FURTHER WORK

Comparison with the measurements on the Cumpsty-Head wing show that:

(i) Present turbulent boundary-layer methods do not predict the flow in the leading-edge region with sufficient accuracy for design needs.

Further boundary-layer calculations show that:

(ii) Reverse transition seems likely to occur on swept leading edges in flight both at low speed, when medium lift is produced by incidence, and at transonic cruise conditions.

(iii) The effect of reverse transition is to lower the predicted upper surface profile drag by as much as 8% compared with the fully turbulent prediction.

Discussion suggests that:

(iv) Some modern 'peaky' sections are likely to be more susceptible to reverse transition effects. Hence predictions of buffet margins, and other quantities depending on a proper knowledge of the influence of viscosity, require basic experiments to improve understanding of the swept leading-edge flow.

In the Appendix a series of boundary-layer calculations are made for yawed circular cylinders and used to prepare design charts for possible low-speed experiments in which detailed boundary-layer measurement could be made.

(v) It is found that such experiments could be conducted in either the Cambridge University Engineering Laboratory 5ft × 4ft tunnel or (preferably) in the 13ft × 9ft tunnel at RAE Bedford.

(vi) Finally, we may conclude that, following the production of reliable basic data, the simple entrainment method could be improved and calibrated to give higher accuracy for viscous swept wing design.

Acknowledgments

The author thanks Dr. R.C. Lock for his encouragement and support for this work. For assistance in running the computer programs and analysing the considerable amount of output, the author also thanks Miss A.G.J. MacDonald and Mr. M. Ralph.

Appendix

THE USE OF BOUNDARY-LAYER CALCULATIONS TO DESIGN A SWEPT LEADING-EDGE EXPERIMENT

The proposed configuration is sketched in Fig.11. A circular cylinder is used as it can be very accurately made and also permits the traverse gear to be housed internally as shown. This avoids the interference with the external flow that was encountered by Cumpsty and Head[12] in their experiment. The fairing should be designed to produce an aerofoil section with a smaller thickness-chord ratio than that of Cumpsty and Head's wing in order to avoid rear separation and possible unsteadiness of the mean flow.

Boundary-layer calculations using the entrainment method[4] have been made, using the analytical expression for potential flow around a circular cylinder, for a wide range of radius Reynolds numbers,

$$10^5 \leqslant R_R \left(= \frac{U_\infty}{\nu_\infty} R\right) \leqslant 10^7 \quad ,$$

and sweep angles $20^\circ \leqslant \Lambda \leqslant 70^\circ$, as shown in Fig.12 where the contours of equal lengths (L_{RT}/δ_{AV}), along external streamlines, of the region of laminar reversion $(\Delta_{1s} \leqslant -0.01)$ are shown.

The conditions to be satisfied in the design of a leading-edge experiment are listed below.

A.1 Physical limitations

$$L_{RT} \geqslant 20\delta_{AV} \text{ over a range of Reynolds numbers,} \qquad \text{(A-1)}$$

in order to ensure that reverse transition is established[20].

The aerofoil chord (c) must probably be larger than 6t to avoid rear separation. Hence,

$$c \geqslant 6t \quad . \qquad \text{(A-2)}$$

A.2 Traverse gear limitations

It is considered that if the boundary-layer thickness (δ) falls below 0.1 in, precise measurements of the flow direction within the inner region of the boundary layer will become impossible. Hence the first condition to be satisfied is

$$\delta_{min} \geqslant 0.1 \text{ in} \quad . \qquad \text{(A-3)}$$

Fig.15 shows δ_{min}/R as a function of sweep angle (Λ) with the small dependency (over the permissible range at each Λ) on Reynolds number ignored, as uncertainties in defining boundary-layer thickness are dominant.

Of lesser importance but still worth consideration is the total rotation that the traverse gear will require in order to align the yaw probe with the boundary-layer flow direction everywhere from the attachment line to the position of peak velocity. The flow at the leading edge lies along the generator and is at right angles to the chordal plane. Downstream the surface flow makes an angle of $(\phi + \beta)^o$ with the chordal plane. Hence the change of angle is $(90 - \phi - \beta)^o$. The maximum value of this rotation is plotted, in Fig.16, as

$$\Delta\varepsilon = (90 - \phi - \beta)^o_{max} . \qquad \text{(A-4)}$$

A.3 Probe limitations

Maximum local freestream velocity of

$$U_e = 300 \text{ ft/s} \qquad \text{(A-5)}$$

can be assumed for a satisfactory life of the hot-wire probes. A minimum local velocity inside the boundary layer for accurate mean velocity measurements with hot-wire or flattened pitot probes can reasonably be assumed as

$$u(y) = 20 \text{ ft/s} . \qquad \text{(A-6)}$$

Hence, the minimum desirable value of external velocity is, approximately,

$$U_e = 50 \text{ ft/s} \qquad \text{(A-7)}$$

A.4 Wind tunnel limitations

A maximum speed of

$$U_\infty = 250 \text{ ft/s} \qquad \text{(A-8)}$$

was considered desirable if steady running was to be obtained with existing low speed wind tunnels.

Blockage to the flow limits the aerofoil thickness (t) to about one-third of the height (H) of the working section (see Fig.17). If $R = t/2$, this gives,

$$R \leqslant H/6 \ . \tag{A-9}$$

In Fig.12, the boundaries corresponding to conditions (A-5), (A-6) and (A-9) together with a maximum desirable sweep (Λ) of 70° are shown for cylinder radii of

$$R = 3 \text{ in}, \ 6 \text{ in}, \text{ and } 12 \text{ in} \ .$$

From the sketch, in Fig.17, we can deduce the condition that follows from (A-9) and (A-2), relating tunnel working section dimensions to wing sweep.

The total length of usable working section is L and so we have,

$$L \geqslant c + W \tan \Lambda \ , \tag{A-10}$$

$$\text{or} \quad L \geqslant 6t + W \tan \Lambda, \text{ from (A-2)} \ , \tag{A-11}$$

$$\text{or} \quad L \geqslant 12R + W \tan \Lambda \ , \tag{A-12}$$

where W is the tunnel width.

Finally, as shown by the sketches of Fig.18, the end fairings, required to ensure a satisfactory extent of 'infinite' wing flow, extend by an amount ψ across the flow. To prevent undue blockage in the wing plane we assume that,

$$\psi \leqslant 0.2W \ . \tag{A-13}$$

From Fig.18,

$$\frac{\psi}{c'} \simeq \frac{0.2 \ \Lambda^{\circ}}{60} ,$$

using the results of calculations for flow over the section of the Cumpsty-Head wing. From (A-13)

$$\frac{W}{c'} = \frac{\Lambda^{\circ}}{60} ,$$

Hence,

$$W = c \frac{\Lambda^{\circ}}{60} \cos \Lambda \ ,$$

and from (A-2),

NOTATION

c	chord length in line of flight
c'	chord length normal to generators
C^*	$= \dfrac{U_\infty^2 \sin^2 \Lambda}{\nu_{a.l.}\, dU_1/ds'}$, attachment-line parameter
C_D, C_L	conventional drag, lift coefficients
F	entrainment coefficient
H	height of wind-tunnel working section (used only in the Appendix)
H_1	$= (\delta - \delta^*)/\theta_{11}$ } conventional boundary-layer shape factors
H_{11}	$= \delta^*/\theta_{11}$ } conventional boundary-layer shape factors
L	useable length of working section of a wind tunnel
L_{RT}	length, measured along the path of an external streamline, of the region of reverse transition
M	Mach number (e.g. M_e, M_∞)
p	local static pressure
R	radius of cylinder
R_c	$= \dfrac{U_\infty c}{\gamma_\infty}$, streamwise (line of flight) chord Reynolds number
$R_{c'}$	$= \dfrac{U_\infty \cos \Lambda\, c'}{\gamma_\infty} = R_c \cos^2 \Lambda$
R_R	$= \dfrac{U_\infty R}{\nu_\infty}$, cylinder radius Reynolds number
R_0	$= R/\cos^2 (\phi + \beta)$, surface radius of curvature in plane of $\underline{\tau_w}$, for a yawed circular cylinder
$R_{\theta_{11}}$	$= \dfrac{U_e \theta_{11}}{\nu_e}$
s	distance along an external streamline started at a small distance ε from the attachment line
s'	distance, in the chordwise plane, around the surface from the attachment line
t	aerofoil thickness
U_e	local external velocity

NOTATION (continued)

U_1	component of U_e in chordwise direction
U_∞	freestream velocity far upstream
U_{1_∞}	$= U_\infty \cos \Lambda$
U_τ	local friction velocity $\left(= \sqrt{\frac{\tau_w}{\rho_w}} \right)$

Planform coordinate systems:

x', y', z'	rectangular Cartesian coordinates with x' chordwise, y' spanwise, z' normal to wing plane For local boundary layer expressions we use rectangular coordinates with z normal to the surface and either s or s' with the appropriate third normal coordinate (y or y')
W	width of wind-tunnel working section (see the Appendix)
α	angle of incidence
β	angle between $\underline{\tau_w}$ and $\underline{U_e}$
δ	value of z for which the total velocity in boundary layer $= 0.995U_e$
$\bar{\delta}$	$= \int_0^\delta \frac{\rho}{\rho_e} dz$
δ_{min}	smallest thickness of boundary layer for which satisfactory yawprobe traverses can be made (see Appendix - section A.2)
δ^*	boundary-layer displacement thickness
Δ_1, Δ_{1s}	inner region pressure gradient parameters
$\Delta\varepsilon$	angle of rotation of traverse gear (see Appendix)
Λ	angle of yaw of wing
η	transformed y-coordinate of boundary layer
ρ	fluid density
σ'	effective leading-edge radius (i.e. the radius of the circular cylinder that, in incompressible flow, has the same velocity gradient as at the attachment line of the aerofoil) of the chord-wise section, used to find C^*
ϕ	angle between $\underline{s'}$ and $\underline{U_e}$ vectors
ν	fluid kinematic viscosity

NOTATION (concluded)

θ_{11}	$= \int_0^s \frac{\rho_u}{\rho_e U_e}\left(1 - \frac{u}{U_e}\right) dz$, conventional streamwise profile momentum loss thickness
ψ	lateral displacement of an external streamline (see Fig.18)
τ_w	wall shear stress

Subscripts;

AV	value averaged over a given streamwise length of boundary-layer development
a.l.	value at attachment line
u	value for aerofoil or wing upper surface
w	value at surface of wing

Superscript:

'	value using quantities in the x',y'z' coordinate system

REFERENCES

No.	Author	Title, etc
1	N.A. Cumpsty M.R. Head	The calculation of three-dimensional turbulent boundary layers. Part 3 Comparison of attachment-line calculations with experiment. Aero Quart Vol.20, Part 2, pp.99-113 (1969)
2	N.A. Cumpsty M.R. Head	The calculation of three-dimensional turbulent boundary layers. Part 1 Flow over the rear of an infinite swept wing. Aero Quart Vol.18, Part 1, pp.55-84 (1967)
3	P. Bradshaw	Calculation of three-dimensional turbulent boundary layers. J.F.M., Vol.46, Part III, pp.417-445 (1971)
4	B.G.J. Thompson A.G.J. Macdonald	The prediction of boundary-layer behaviour and profile drag for infinite yawed wings. Part I, A method of calculation. ARC CP No.1307 (1973)
5	L. Rosenhead (ed.)	Laminar boundary layers. Oxford University Press (1963)
6	M. Gaster	On the flow along swept leading edges. Aero Quart Vol.18, p.165 (1967)
7	W. Pfenninger	Flow phenomena at the leading edge of a swept wing. AGARDograph 97, Recent developments in boundary-layer research, Part 4 (1965)
8	N. Gregory E.M. Love	Laminar flow on a swept leading edge: final progress report. NPL Aero Memorandum 26, ARC 27979 (1965)
9	N.A. Cumpsty M.R. Head	The calculation of three-dimensional turbulent boundary layers. Part 2 Attachment-line flow on an infinite swept wing. Aero Quart Vol.18, Part 2, pp.150-164 (1967)

REFERENCES (continued)

No.	Author	Title, etc.
10	J.F. Nash	The calculation of three-dimensional turbulent boundary layers in incompressible flow. J.F.M. Vol.37, Part 4, pp.625-642 (1969)
11	D.F. Myring	An integral prediction method for three-dimensional turbulent boundary layers in incompressible flow. RAE Technical Report 70147 (ARC 32647) (1970)
12	N.A. Cumpsty M.R. Head	The calculation of three-dimensional turbulent boundary layers. Part 4 Comparison of measurement with calculations on the rear of a swept wing. ARC CP No.1077. Aero Quart Vol.21, Part 2, pp.121-132 (1970)
13	P. Bradshaw M.G. Terrell	The response of a turbulent boundary layer on an 'infinite' swept wing to the sudden removal of pressure gradient. NPL Aero Report 1305, ARC 31514 (1969)
14	R.E. Wallace	The experimental investigation of a swept wing research model boundary layer. University of Wichita, School of Engineering, Aero Dept, Report No.092 (1953)
15	G.G. Brebner L.A. Wyatt	Boundary layer measurements at low speed on two wings of 45^o and 55^o sweep. ARC CP No.554 (1961)
16	B.G.J. Thompson G.A. Carr-Hill M. Ralph	The prediction of boundary-layer behaviour and profile drag for infinite yawed wings. Part III, Calculations for a particular wing. ARC CP No.1309 (1973)
17	B.G.J. Thompson G.A. Carr-Hill B.J. Powell	A programme of research into the viscous aspects of flow on swept wings. NPL Aero Note 1100, ARC 32402 (1970)
18	M.G. Hall	Scale effects in flows over swept wings. RAE Technical Report 71043 (ARC 33069) (1971)

REFERENCES (concluded)

No.	Author	Title, etc.
19	V.C. Patel	Calibration of the Preston tube and limitations of its use in pressure gradients. J.F.M. Vol.23, pp.185-208 (1965)
20	B.E. Launder	Laminarisation of the turbulent boundary layer by acceleration. M.I.T. Gas Turbine Lab Report No.77 (1964)
21	M.R. Head	Entrainment in the turbulent boundary layer. ARC R&M 3152 (1960)
22	J.E. Green	The prediction of turbulent boundary-layer development in compressible flow. J.F.M. Vol.31, Part 4, pp.753-778 (1968)
23	H.C. Garner D.E. Walshe	Pressure distribution and surface flow on 5% and 9% thick wings with curved tip and 60° sweep back. ARC R&M 3244 (1960)
24	P. Bradshaw	The analogy between streamline curvature and buoyancy in turbulent shear flow. J.F.M., Vol.36, Pt.1, pp.177-191 (March 1969)
25	G.Y. Nieuwland	Theoretical design of shock-free, transonic flow around aerofoil sections. Int.Coun.Aero.Sci.paper (66-26), Fifth Congress of ICAS (1966)

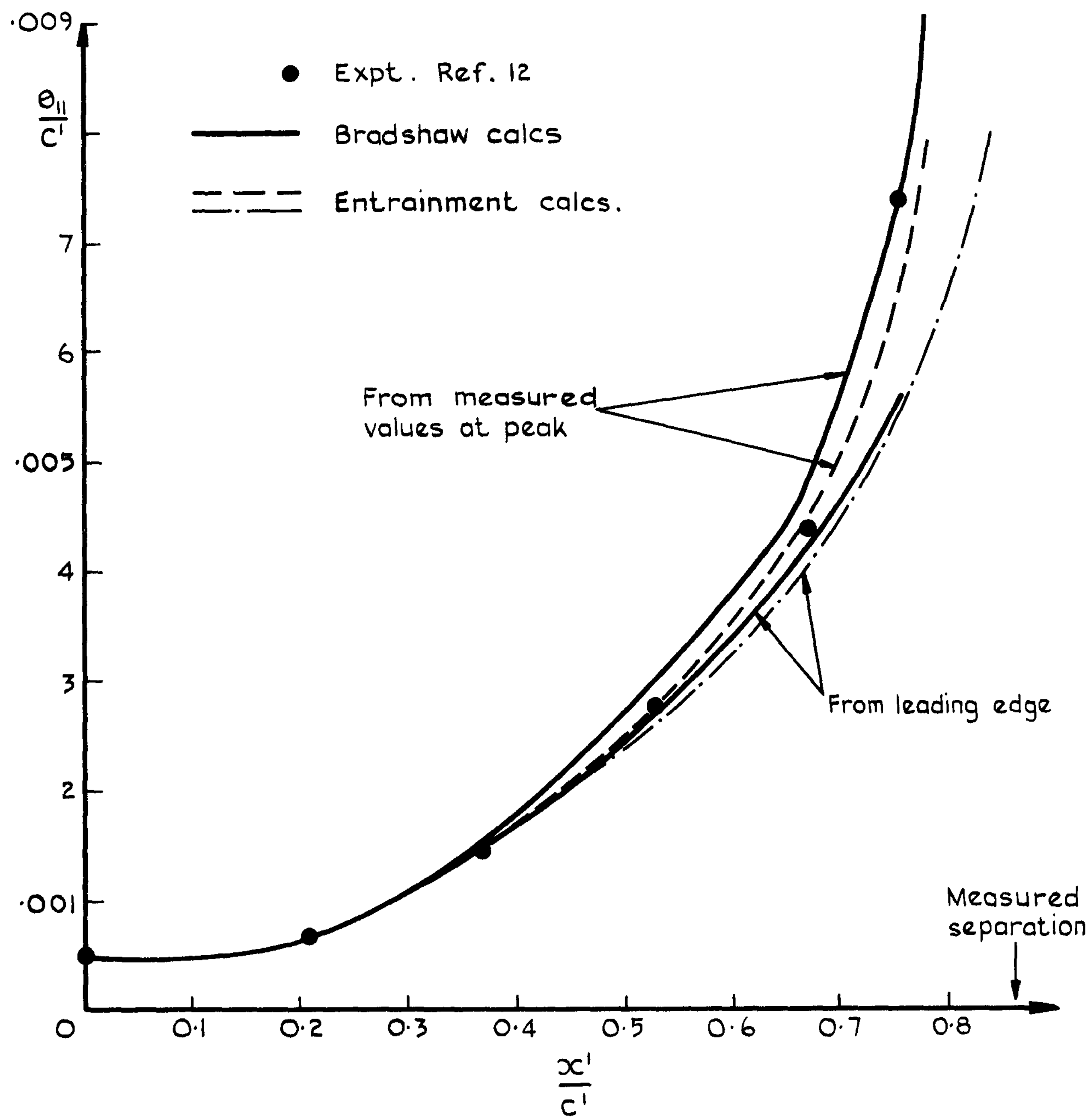

Fig. 1 Development of momentum thickness on Cumpsty – Head 62·5° wing

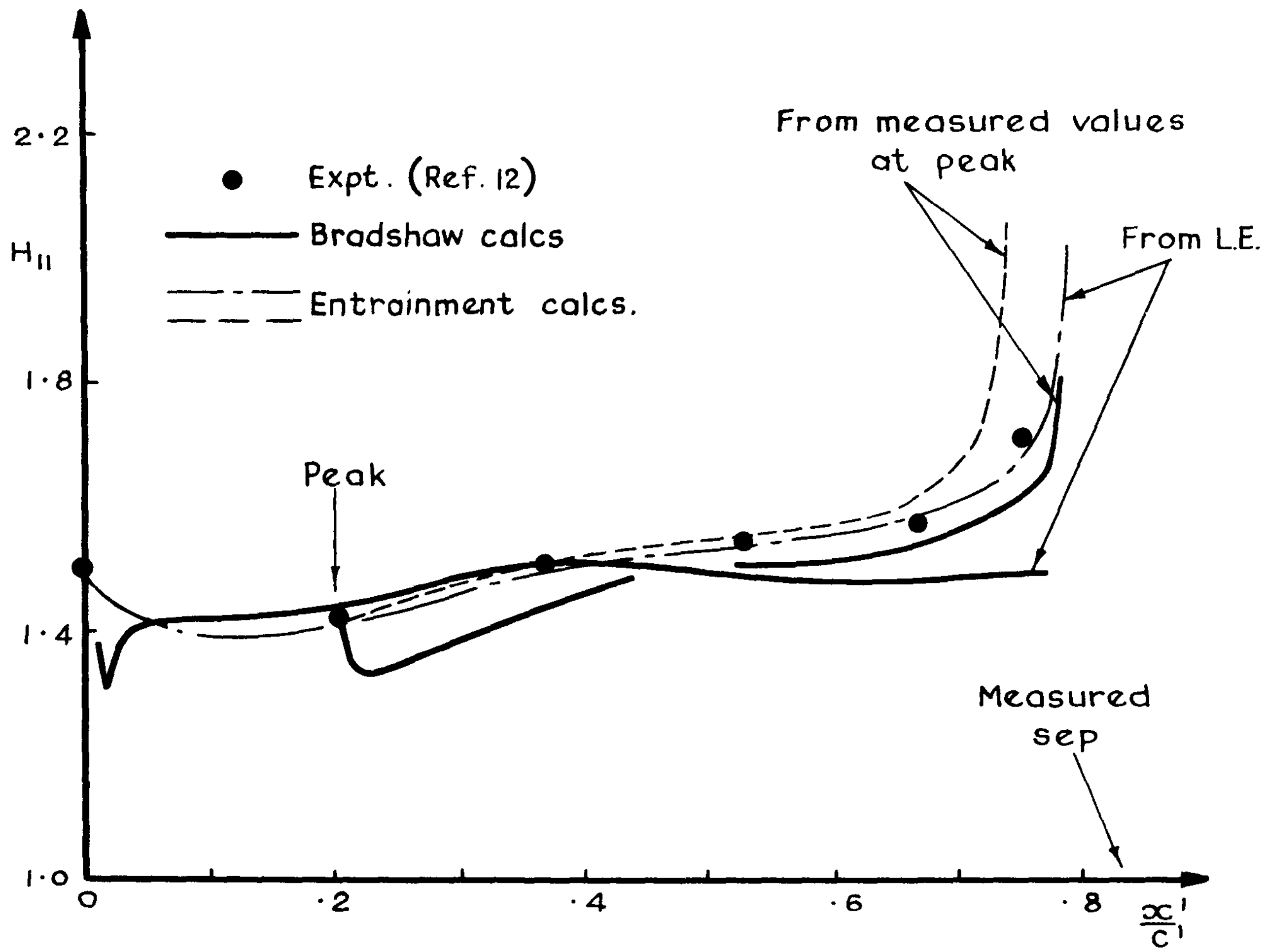

Fig. 2 Development of streamwise profile shape-factor; 62·5° Cumpsty – Head wing

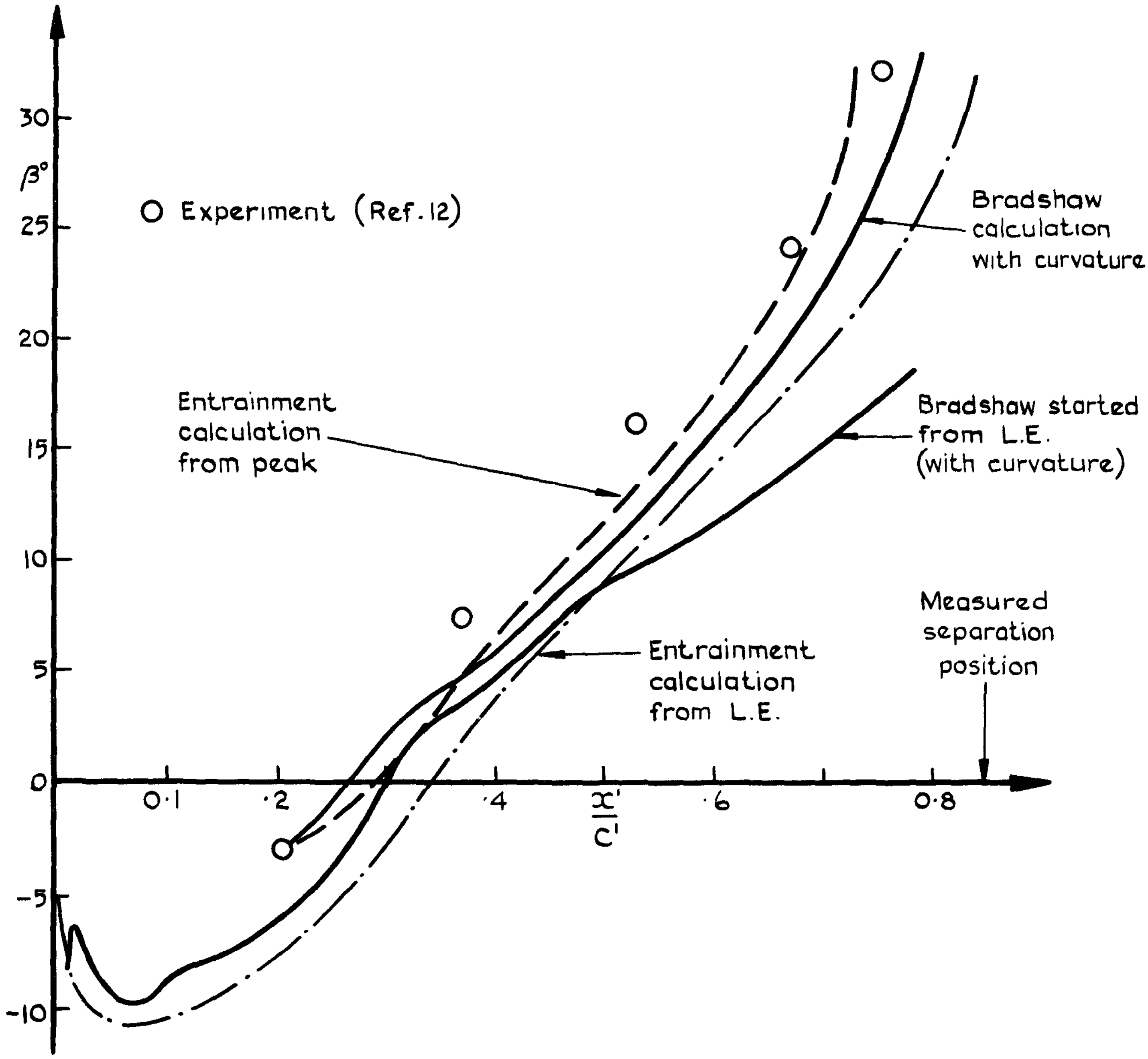

Fig. 3 Development of angle between surface and external streamlines on the 62·5° wing of Cumpsty and Head

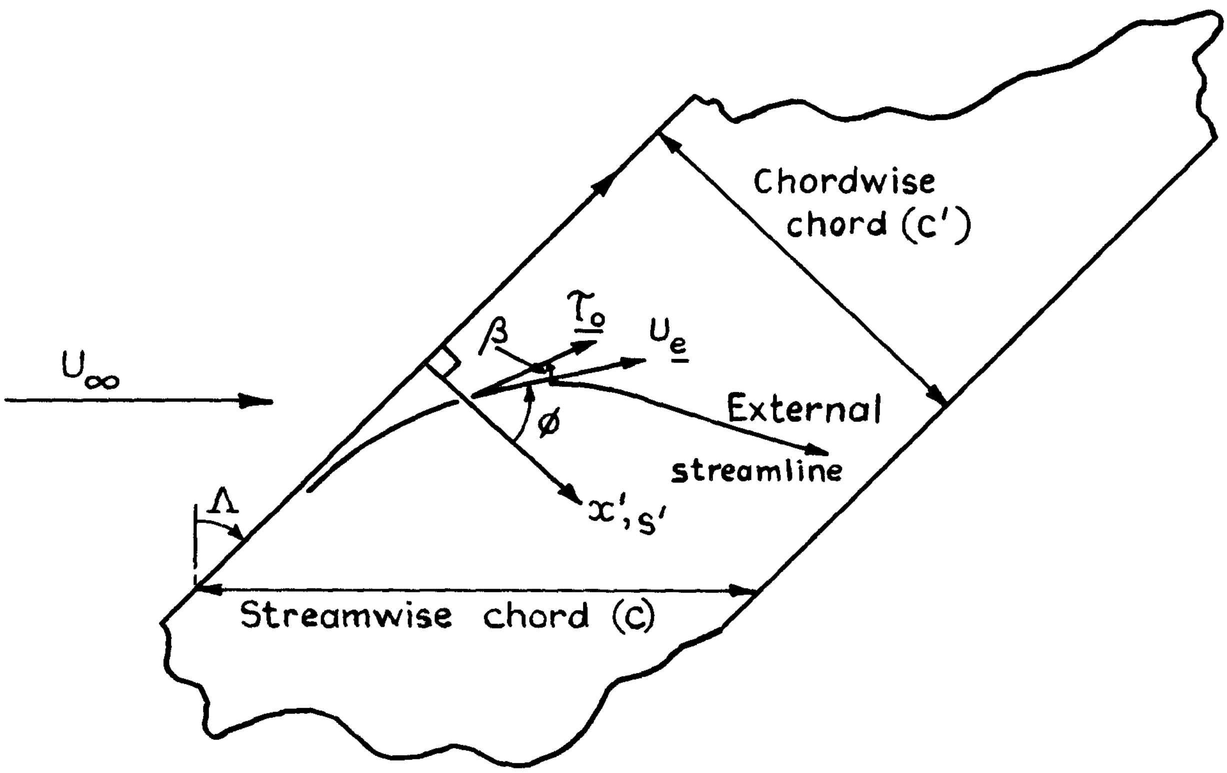

Fig. 4 Definition sketch

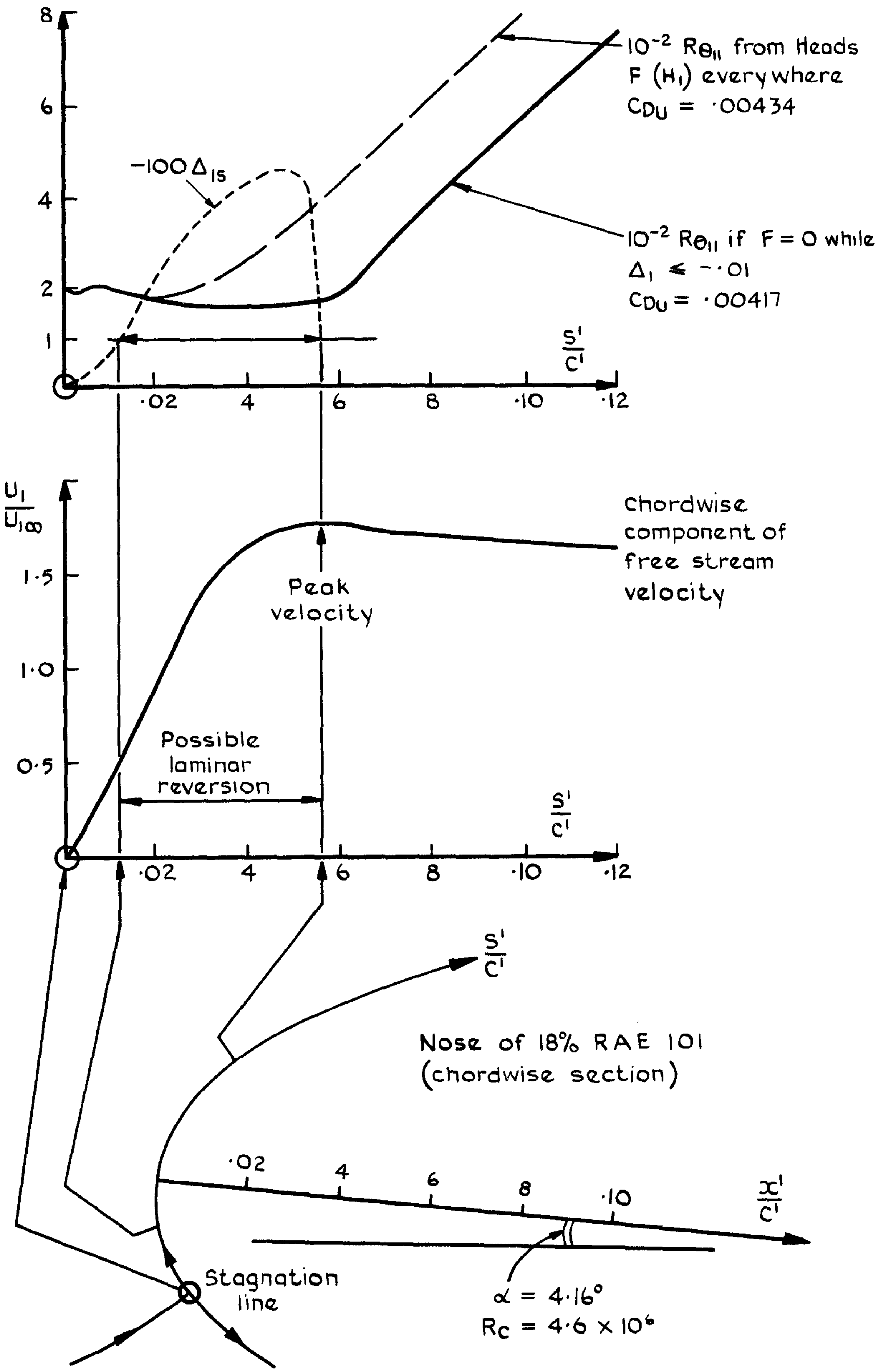

Fig. 5 Possible laminar reversion as predicted around LE of 60° yawed wing

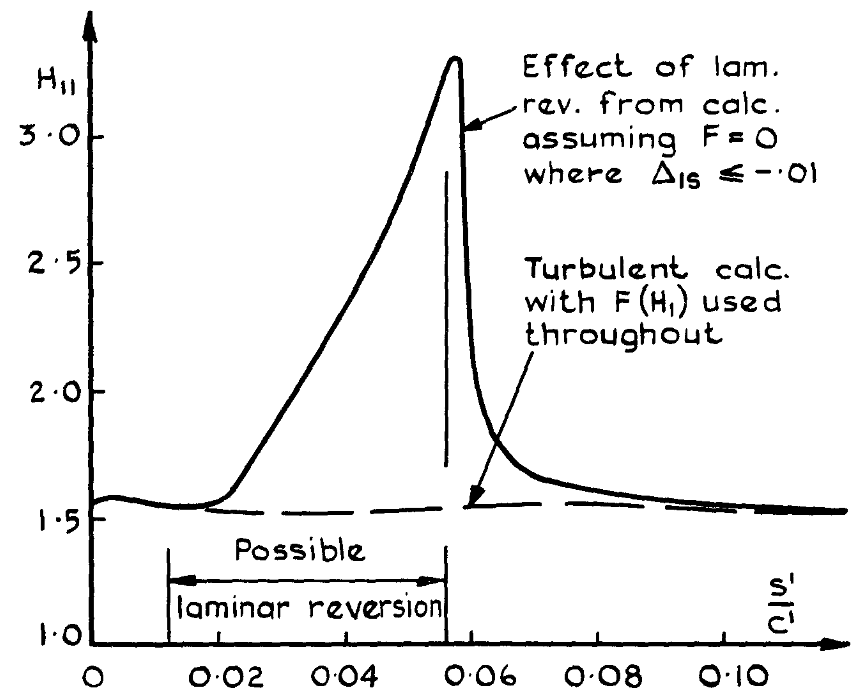

Fig.6 Streamwise profile shape-facter

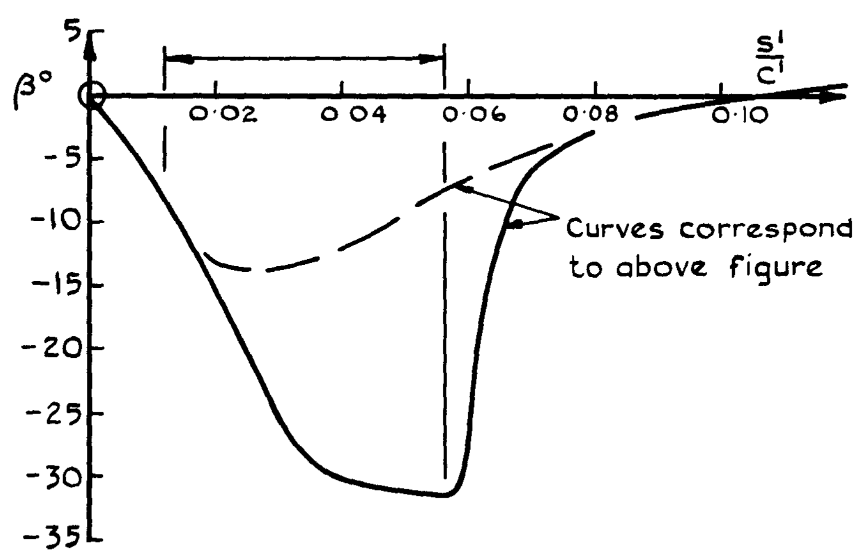

Fig.7 Surface cross-flow angle

Predicted effect of laminar reversion on boundary layer characteristics near a swept leading edge (conditions as for figure 5)

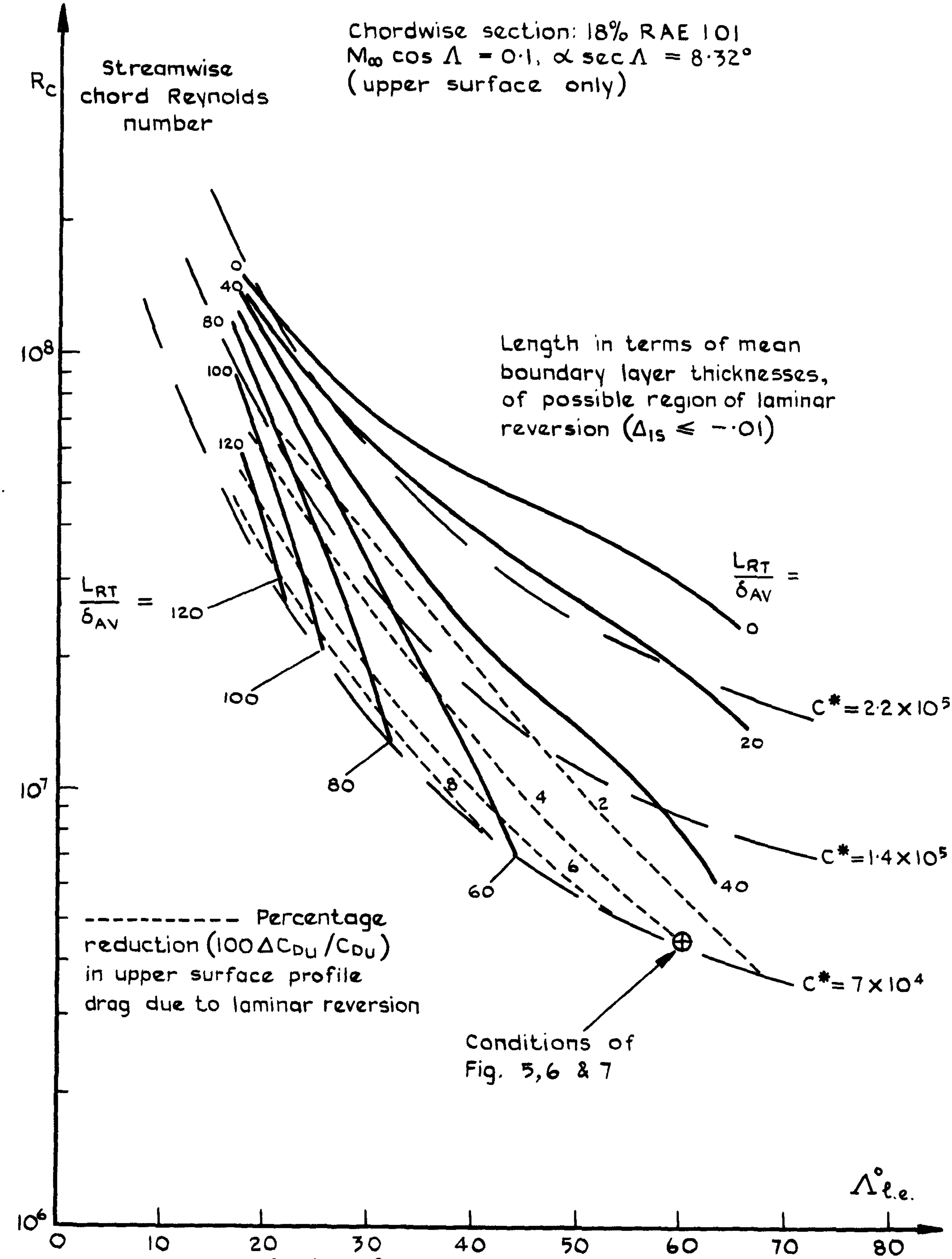

Fig. 8 The effect of laminar reversion upon profile drag predictions for yawed wings having a symmetrical section at incidence

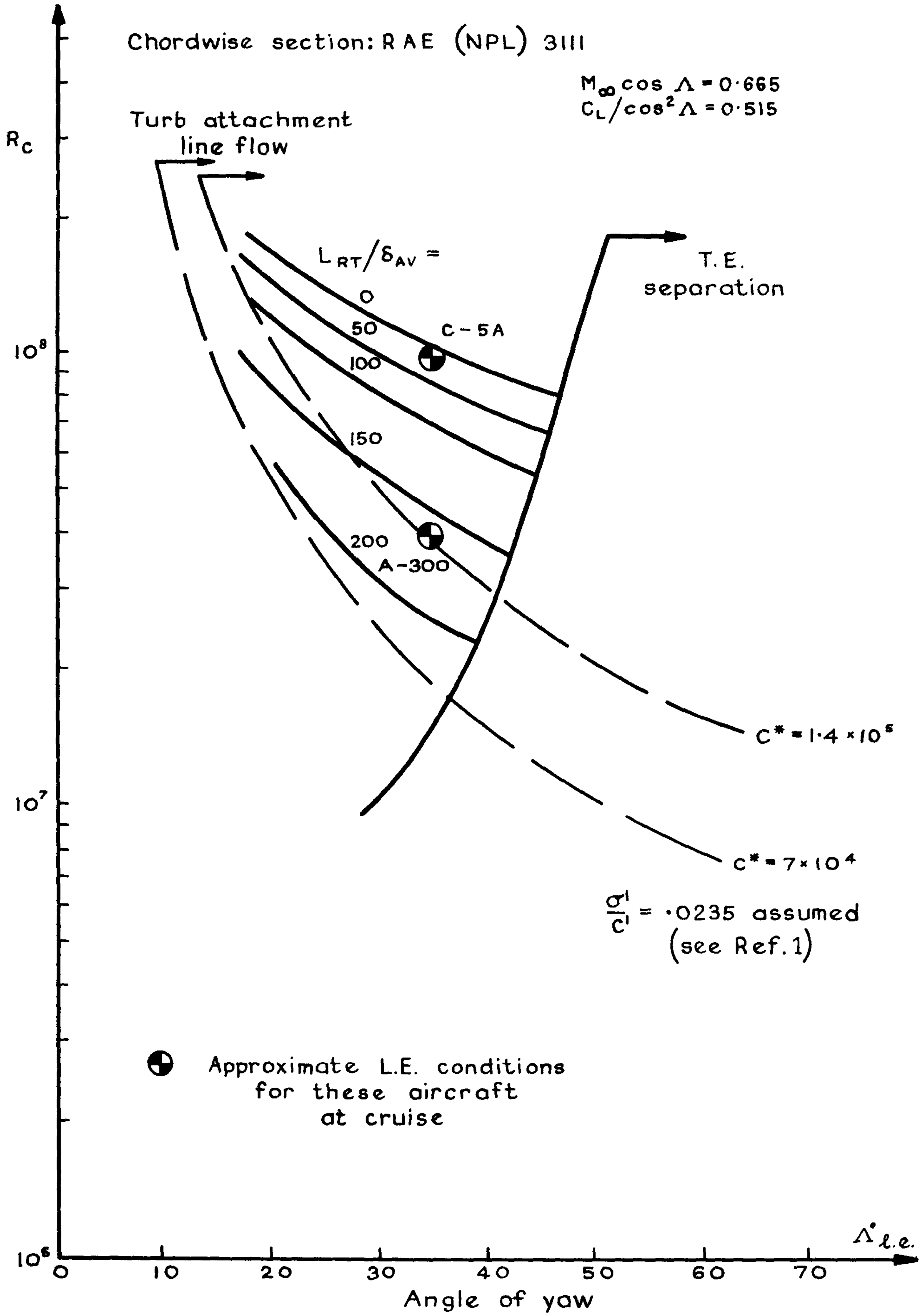

Fig 9 The extent of laminar reversion predicted for representative swept wings at transonic cruise conditions

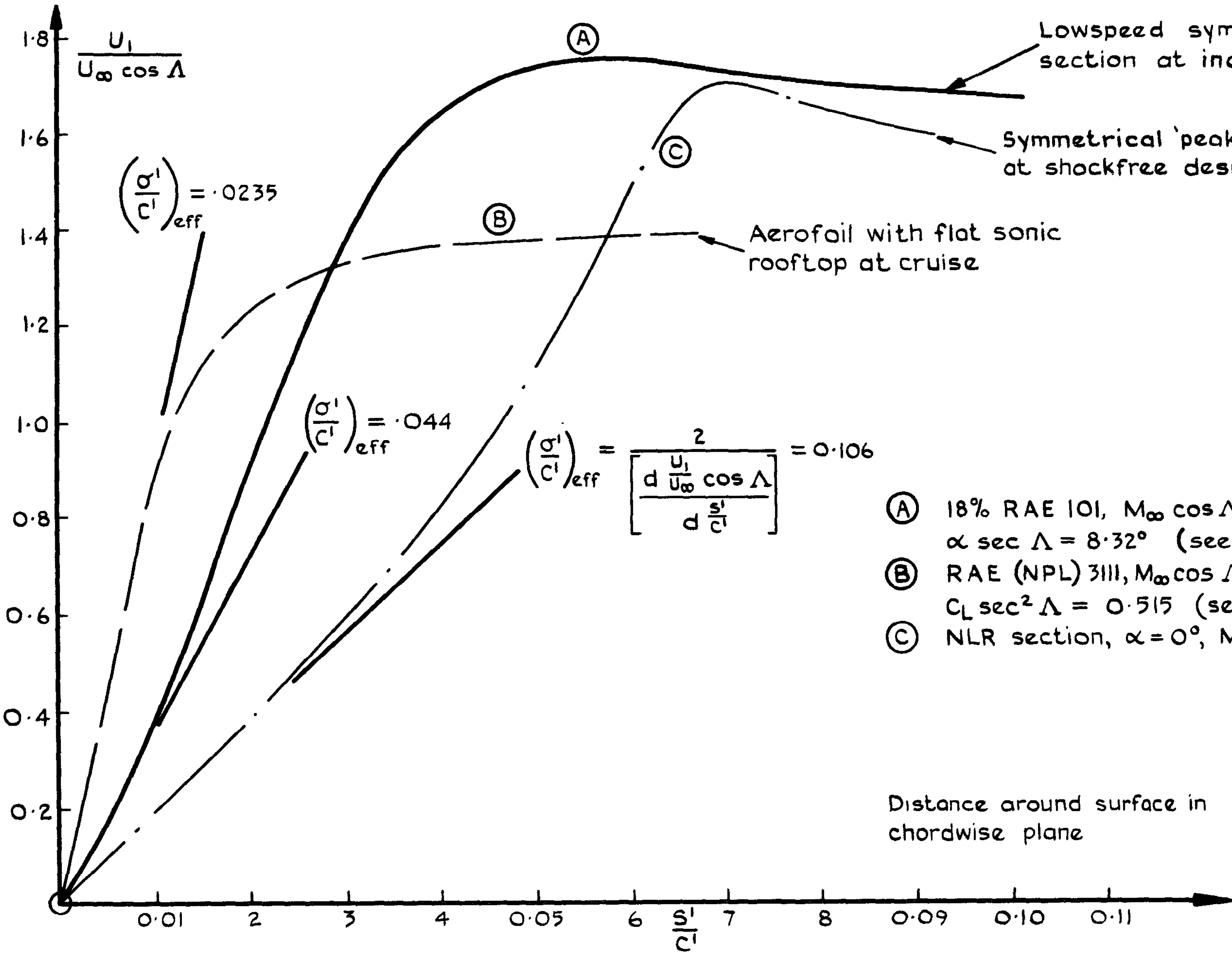

Fig. 10 Comparison of velocity distributions around the leading edges of different types of aerofoils

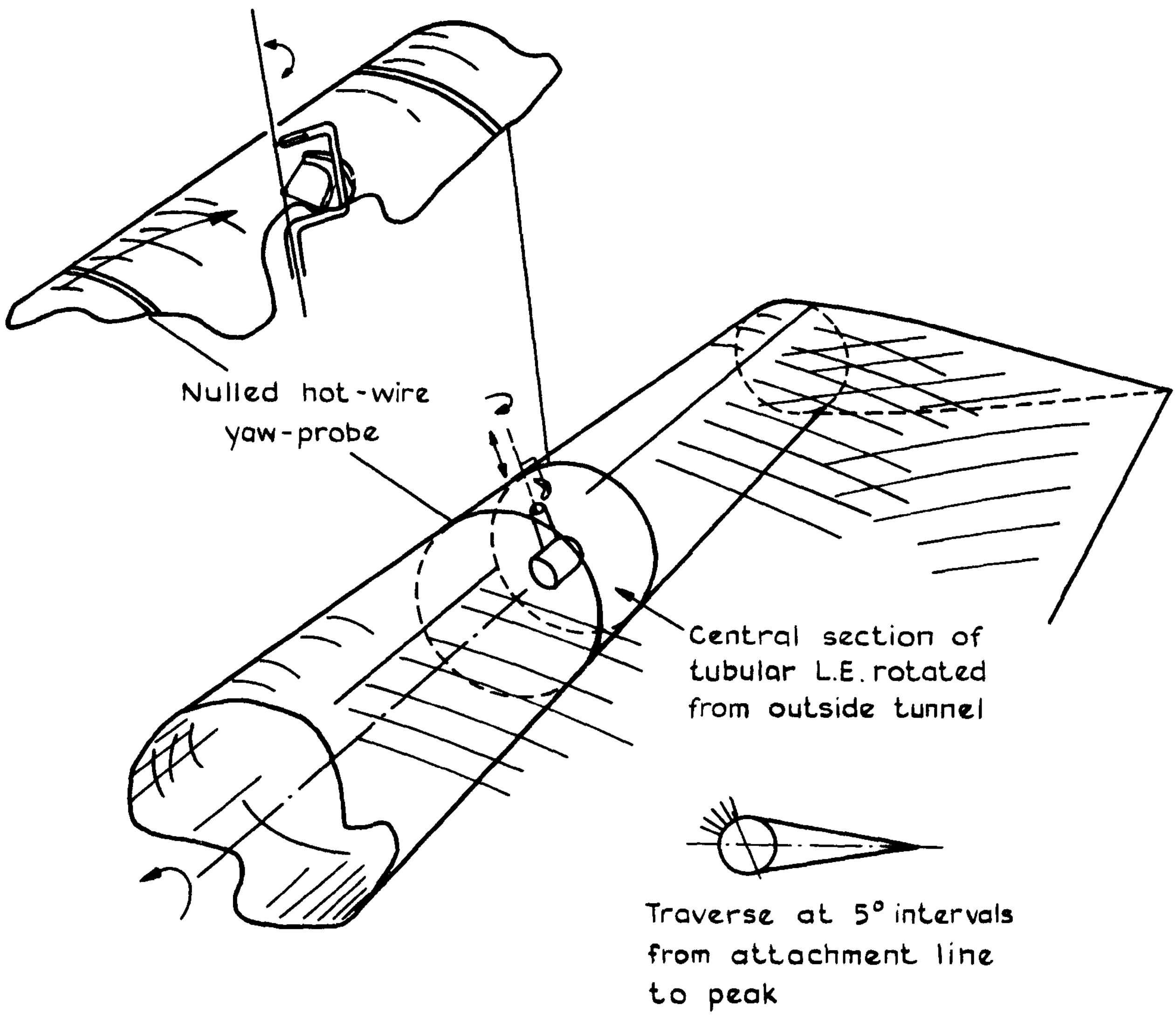

Fig. 11 Yawed leading edge experiment

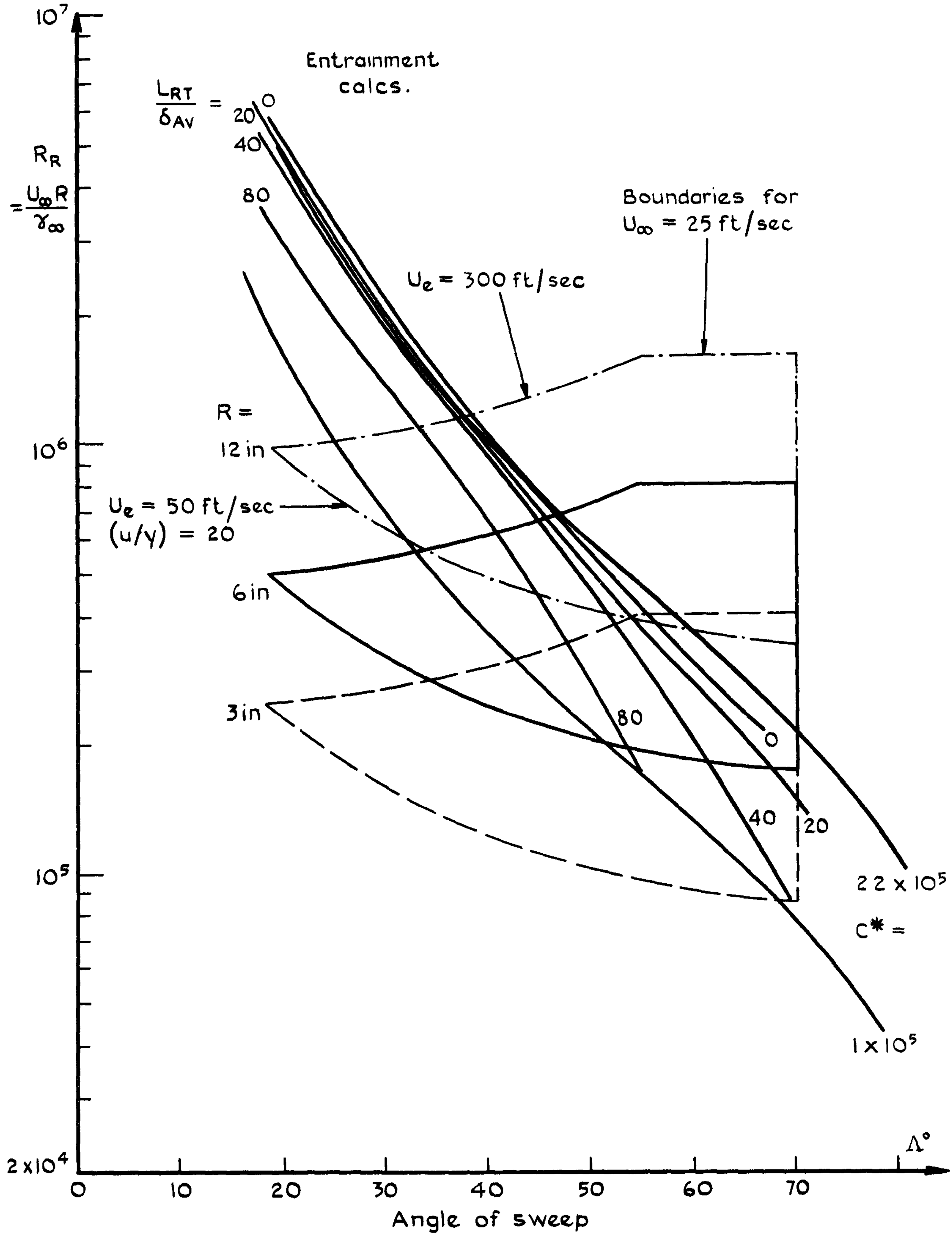

Fig. 12 Length of reverse transition region on yawed circular cylinders

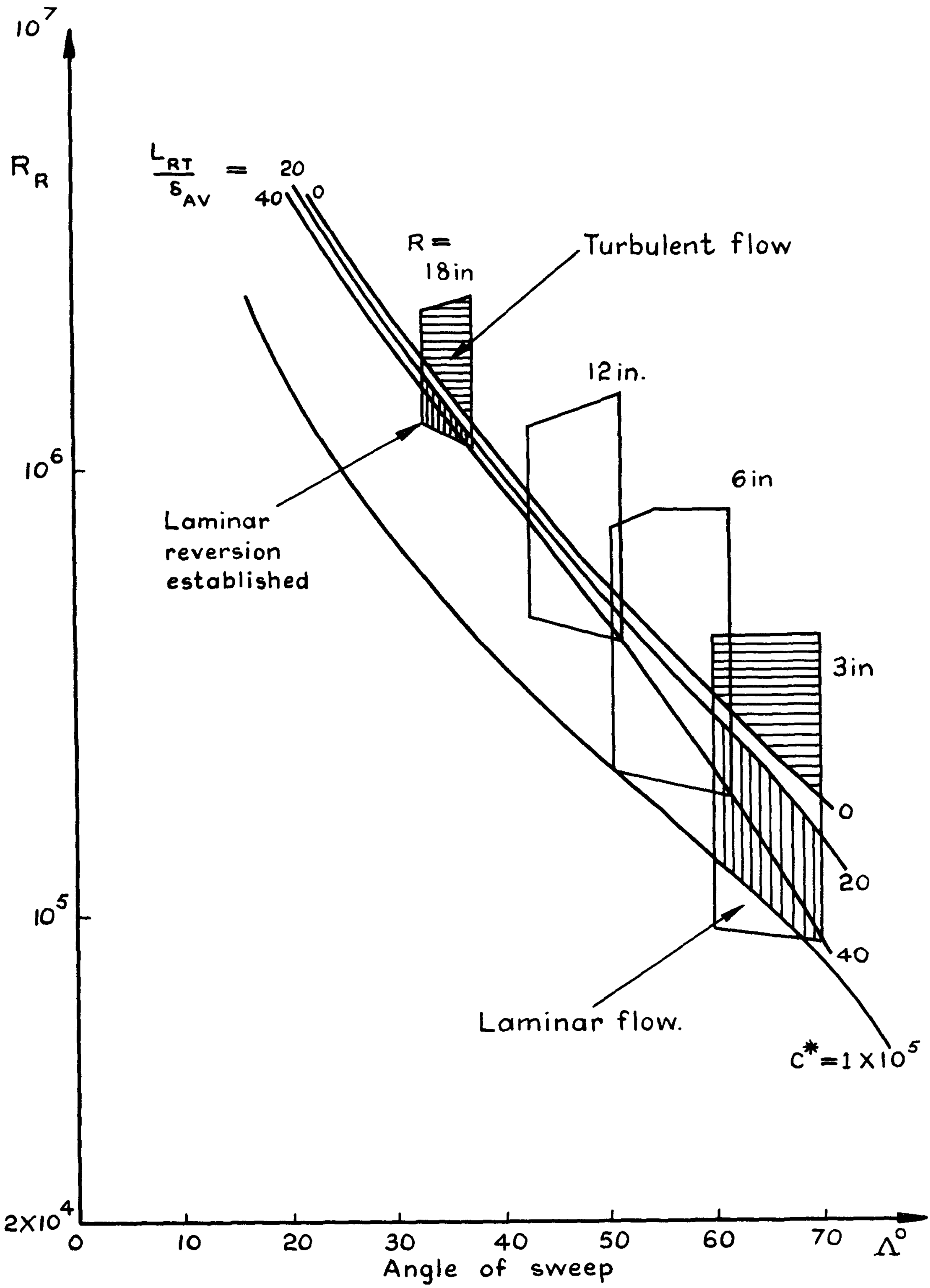

Fig.13 Range of conditions for practical experiments having a coverage both of reverse transition and fully turbulent flow

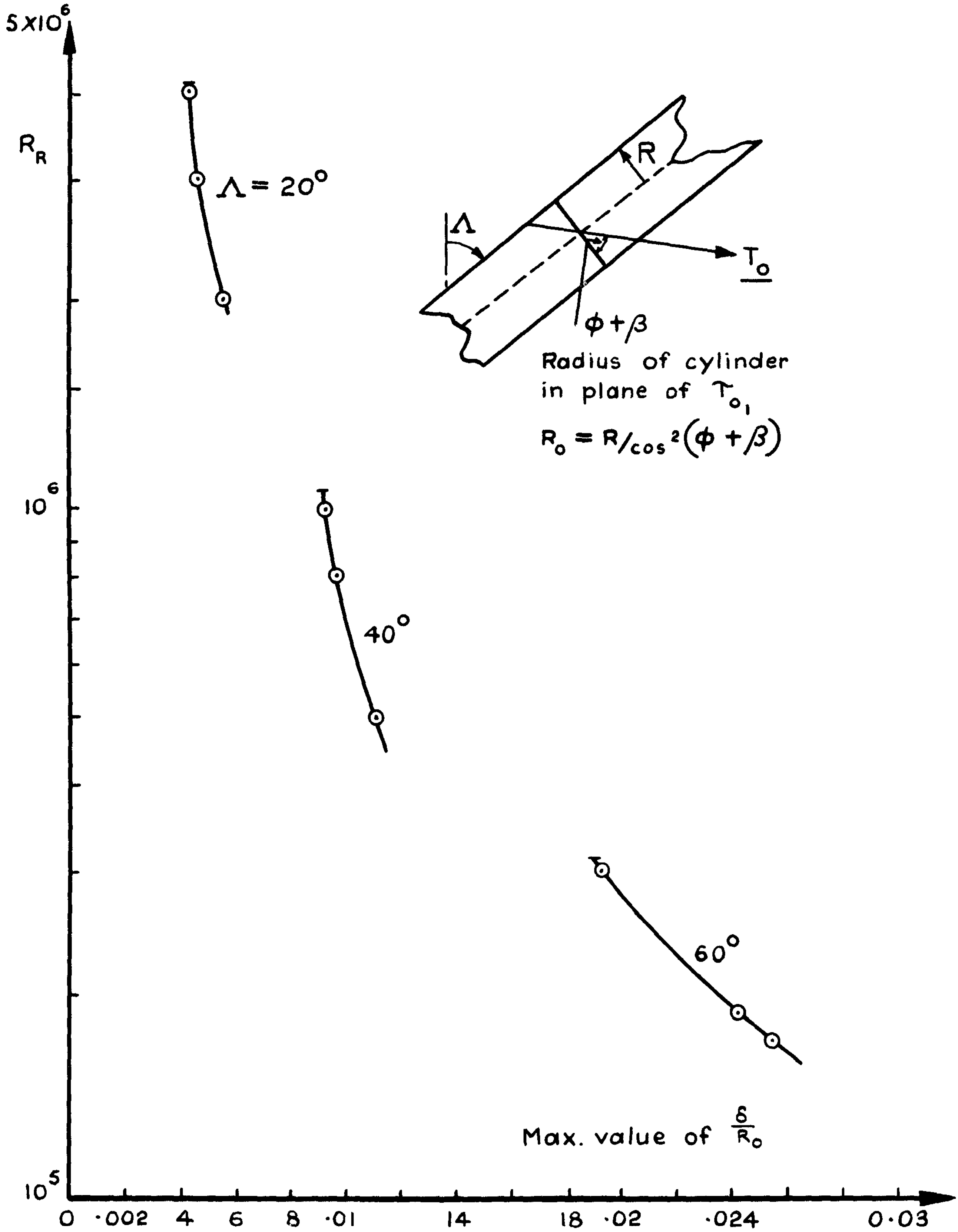

Fig. 14 Curvature parameter in laminar reversion region of flow on swept cirular cylinders

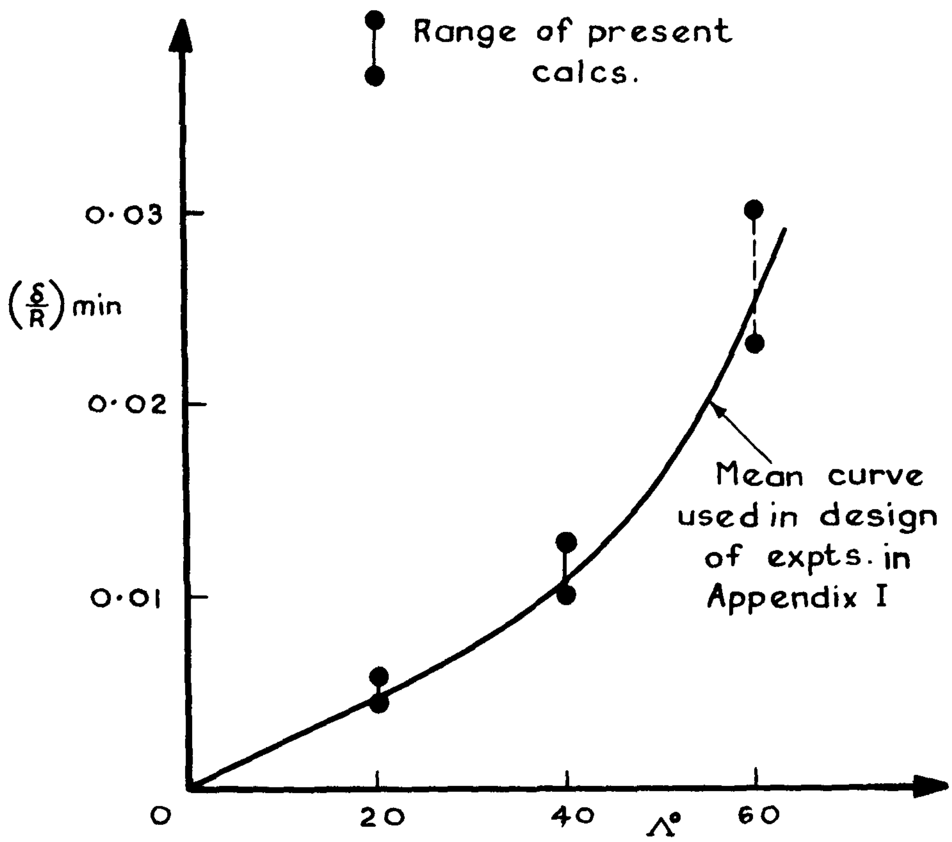

Fig. 15 Approximate variation of the boundary layer minimum thickness (parameter) in the leading edge region of the flow on yawed circular cylinders

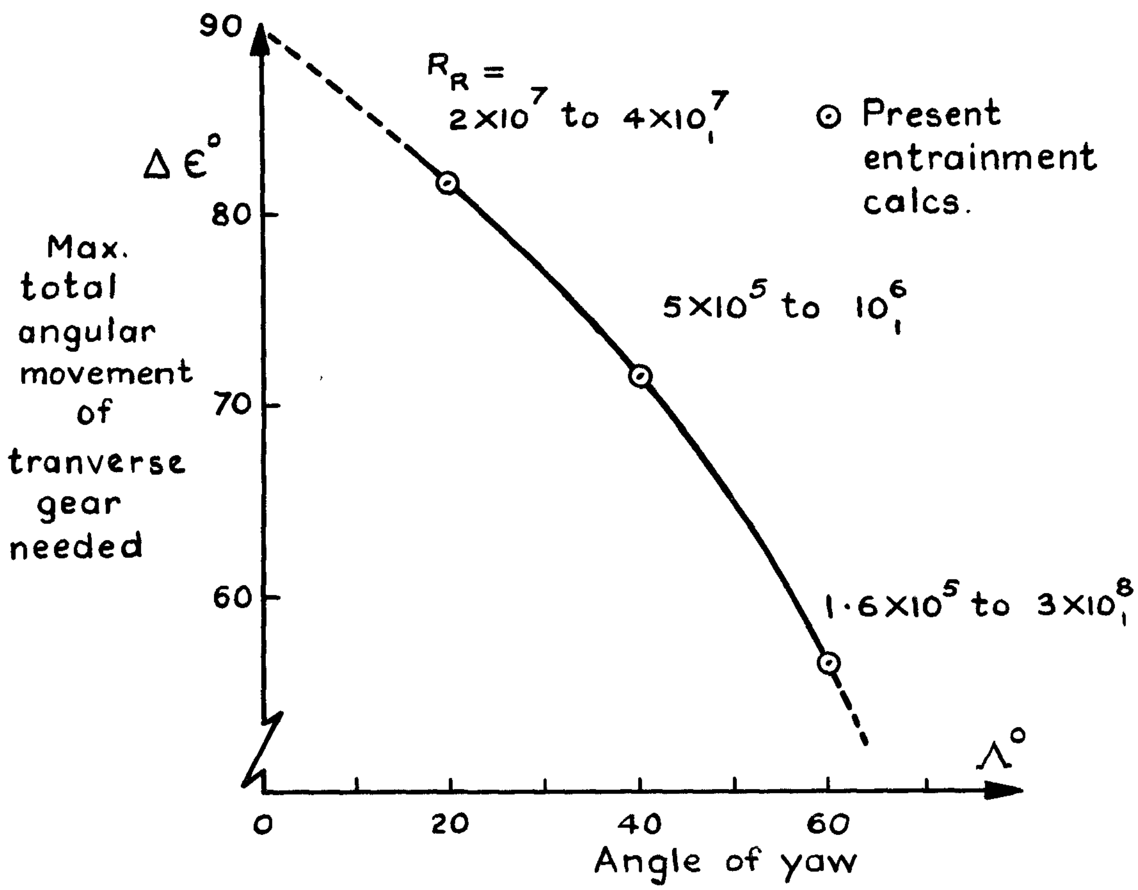

Fig.16 Variation of angular movement needed in boundary layer traverses on yawed circular cylinders

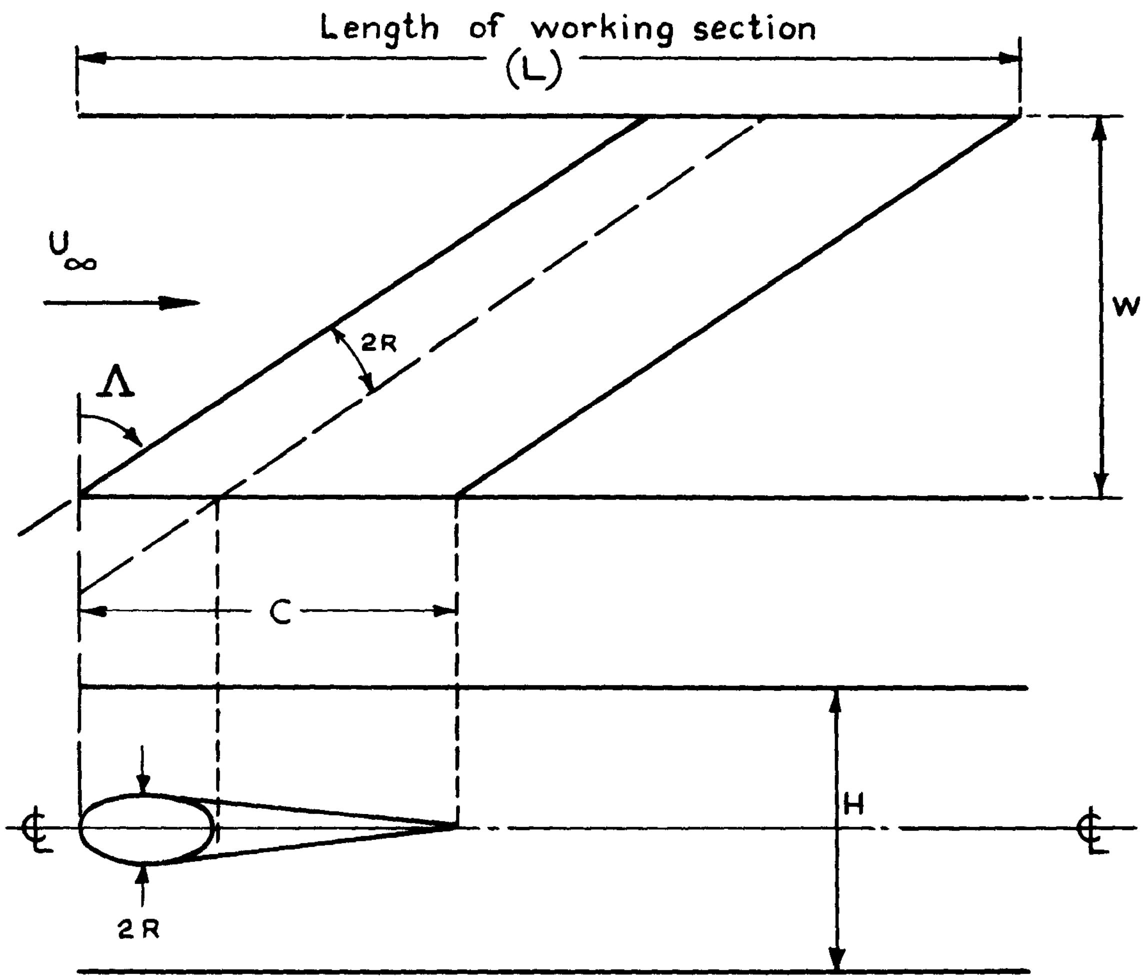

Fig.17 Definition sketches for yawed wing experiment

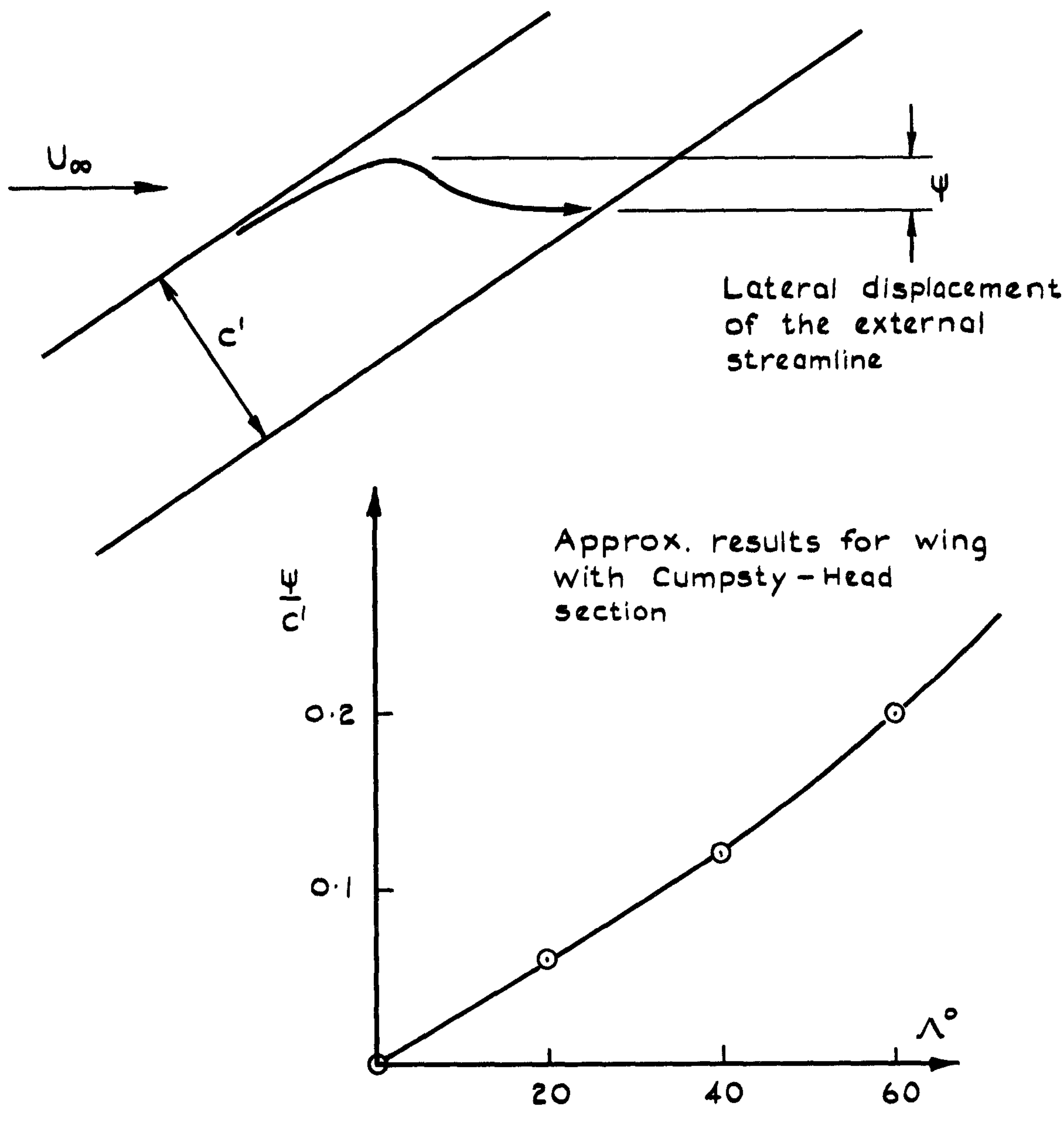

Fig.18 Approximate estimate of size of root fairing required in tunnel expt to ensure adequate span of 'Infinite' yawed wing flow

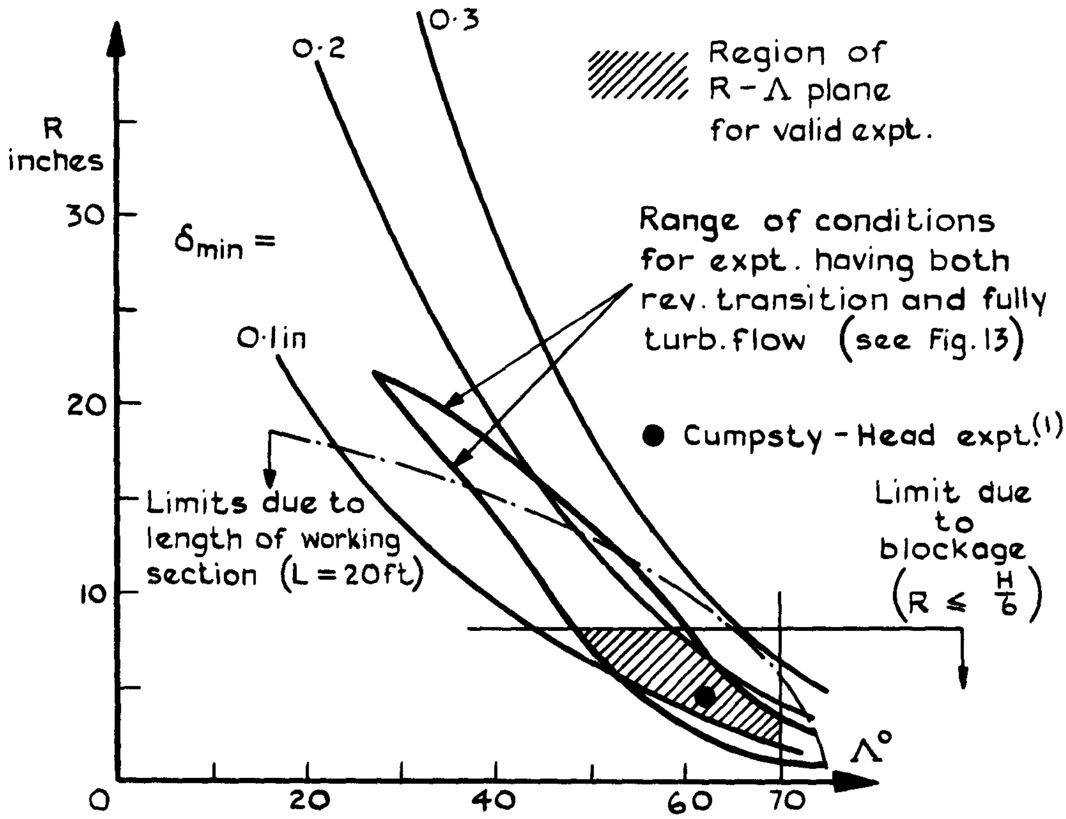

Fig. 19 Results for CUEL 5ft x 4ft tunnel

Conditions for a practical lowspeed investigation of reverse transition downstream of swept leading edges

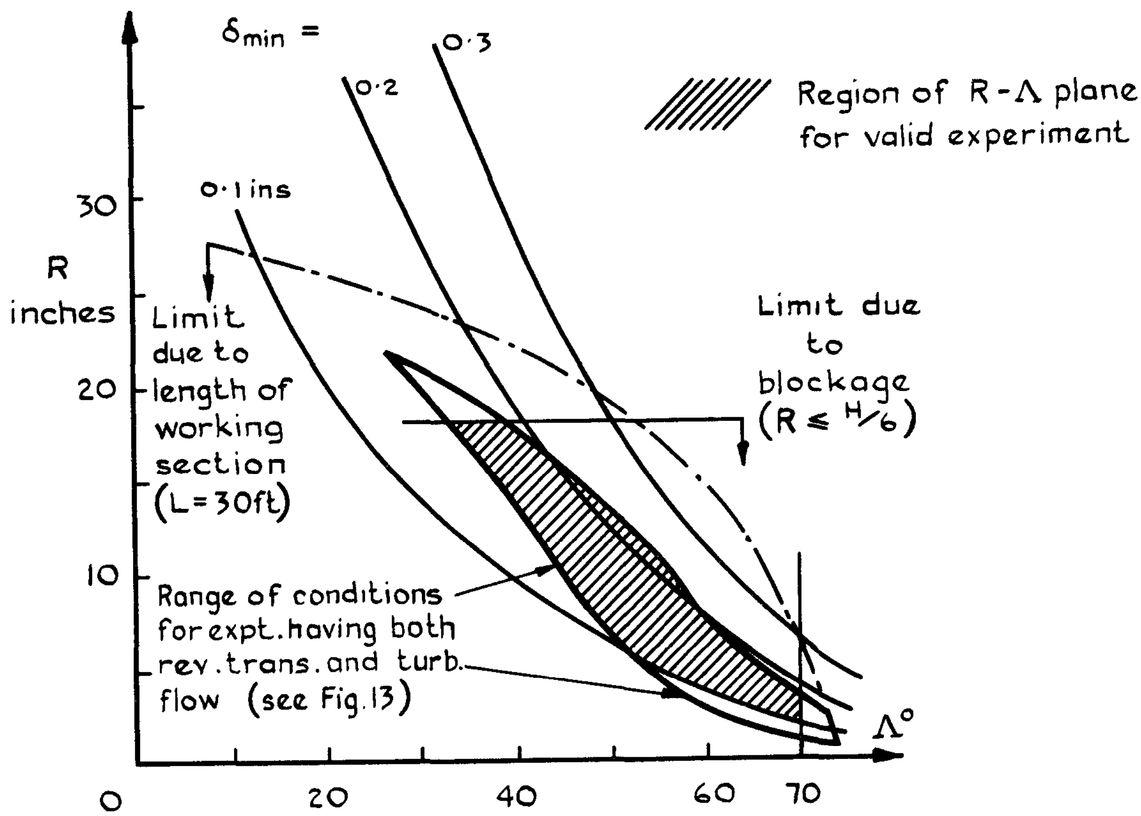

Fig. 20 Results for RAE (Bedford) 13ft x 9ft tunnel

Conditions for a practical lowspeed investigation of reverse transition downstream of swept leading edges

Printed in England for Her Majesty's Stationery Office by the Royal Aircraft Establishment, Farnborough Dd.505376, K4, 11/74.

ARC CP No.1308 | 533.693.1 .
532.526 .
532.526.4 :
533.6.013.122 :
533.6.013.154

May 1973

Thompson, B. G. J.

THE PREDICTION OF BOUNDARY-LAYER BEHAVIOUR
AND PROFILE DRAG FOR INFINITE YAWED WINGS·
Part II FLOW NEAR A TURBULENT ATTACHMENT LINE

In the region of strong favourable pressure gradient between the leading-edge attachment line and the pressure minimum, comparisons with the measurements of Cumpsty and Head, on a 62.5^{o} swept wing, show that current turbulent boundary layer methods do not predict the boundary layer growth accurately enough for practical design applications. Physically, the conditions are severe as there are strong cross-flows developing in the presence of large wall curvature.

Calculations, using the entrainment method of Ref.4, show that, even at flight Reynolds numbers, a conventional swept wing with turbulent attachment line flow could be affected by a prolonged region of reverse transition. Simple assumptions are used to estimate the effect of this on boundary-layer development. It is found that the profile

(Over)

ARC CP No.1308 | 533.693.1 :
532.526 :
532.526.4 .
533.6.013.122 .
533.6.013.154

May 1973

Thompson, B. G. J.

THE PREDICTION OF BOUNDARY-LAYER BEHAVIOUR
AND PROFILE DRAG FOR INFINITE YAWED WINGS·
Part II FLOW NEAR A TURBULENT ATTACHMENT LINE

In the region of strong favourable pressure gradient between the leading-edge attachment line and the pressure minimum, comparisons with the measurements of Cumpsty and Head, on a 62.5^{o} swept wing, show that current turbulent boundary layer methods do not predict the boundary layer growth accurately enough for practical design applications. Physically, the conditions are severe as there are strong cross-flows developing in the presence of large wall curvature.

Calculations, using the entrainment method of Ref.4, show that, even at flight Reynolds numbers, a conventional swept wing with turbulent attachment line flow could be affected by a prolonged region of reverse transition. Simple assumptions are used to estimate the effect of this on boundary-layer development. It is found that the profile

(Over)

ARC CP No.1308 | 533.693.1 :
532.526 :
532.526.4 :
533.6.013.122 ·
533.6.013.154

May 1973

Thompson, B. G. J.

THE PREDICTION OF BOUNDARY-LAYER BEHAVIOUR
AND PROFILE DRAG FOR INFINITE YAWED WINGS:
Part II FLOW NEAR A TURBULENT ATTACHMENT LINE

In the region of strong favourable pressure gradient between the leading-edge attachment line and the pressure minimum, comparisons with the measurements of Cumpsty and Head, on a 62.5^{o} swept wing, show that current turbulent boundary layer methods do not predict the boundary layer growth accurately enough for practical design applications. Physically, the conditions are severe as there are strong cross-flows developing in the presence of large wall curvature.

Calculations, using the entrainment method of Ref.4, show that, even at flight Reynolds numbers, a conventional swept wing with turbulent attachment line flow could be affected by a prolonged region of reverse transition. Simple assumptions are used to estimate the effect of this on boundary-layer development. It is found that the profile

(Over)

Cut here

DETACHABLE ABSTRACT CARDS

DETACHABLE ABSTRACT CARDS

drag could be affected by several per cent and it is thought that the shock-induced separation and scale effects for 'peaky' transonic aerofoils would be even more susceptible to the presence of laminar reversion and that the use of attachment line criterion for turbulent flow (such as C^*) is inadequate on its own.

Finally, calculations using the same boundary layer method are employed to provide charts from which a basic experiment at low speeds can be designed to investigate these problems on a yawed circular cylinder (suitably faired). Results are provided for the 13ft x 9ft wind tunnel at RAE Bedford and for the 5ft x 4ft wind tunnel at the Cambridge University Engineering Laboratory.

drag could be affected by several per cent and it is thought that the shock-induced separation and scale effects for 'peaky' transonic aerofoils would be even more susceptible to the presence of laminar reversion and that the use of attachment line criterion for turbulent flow (such as C^*) is inadequate on its own.

Finally, calculations using the same boundary layer method are employed to provide charts from which a basic experiment at low speeds can be designed to investigate these problems on a yawed circular cylinder (suitably faired). Results are provided for the 13ft x 9ft wind tunnel at RAE Bedford and for the 5ft x 4ft wind tunnel at the Cambridge University Engineering Laboratory.

drag could be affected by several per cent and it is thought that the shock-induced separation and scale effects for 'peaky' transonic aerofoils would be even more susceptible to the presence of laminar reversion and that the use of attachment line criterion for turbulent flow (such as C^*) is inadequate on its own.

Finally, calculations using the same boundary layer method are employed to provide charts from which a basic experiment at low speeds can be designed to investigate these problems on a yawed circular cylinder (suitably faired). Results are provided for the 13ft x 9ft wind tunnel at RAE Bedford and for the 5ft x 4ft wind tunnel at the Cambridge University Engineering Laboratory.

C.P. No. 1308

© *Crown copyright*

1974

Published by
HER MAJESTY'S STATIONERY OFFICE

Government Bookshops
49 High Holborn, London WC1V 6HB
13a Castle Street, Edinburgh EH2 3AR
41 The Hayes, Cardiff CF1 1JW
Brazennose Street, Manchester M60 8AS
Southey House, Wine Street, Bristol BS1 2BQ
258 Broad Street, Birmingham B1 2HE
80 Chichester Street, Belfast BT1 4JY
Government Publications are also available through booksellers

C.P. No. 1308

ISBN 011 470892 4